Runoff generation in a steep, tropical montane cloud forest catchment on permeable volcanic substrate

Lyssette E. Muñoz-Villers[1,2] and Jeffrey J. McDonnell[1,3]

Received 23 August 2011; revised 2 July 2012; accepted 9 July 2012; published 20 September 2012.

[1] Most studies to date in the humid tropics have described a similar pattern of rapid translation of rainfall to runoff via overland flow and shallow subsurface stormflow. However, study sites have been few overall, and one particular system has received very little attention so far: tropical montane cloud forests (TMCF) on volcanic substrate. While TMCFs provide critical ecosystem services, our understanding of runoff generation processes in these environments is limited. Here, we present a study aimed at identifying the dominant water sources and pathways and mean residence times of soil water and streamflow for a first-order, TMCF catchment on volcanic substrate in central eastern Mexico. During a 6-week wetting-up cycle in the 2009 wet season, total rainfall was 1200 mm and storm event runoff ratios increased progressively from 11 to 54%. With the increasing antecedent wetness conditions, our isotope and chemical-based hydrograph separation analysis showed increases of pre-event water contributions to the storm hydrograph, from 35 to 99%. Stable isotope-based mean residence times estimates showed that soil water aged only vertically through the soil profile from 5 weeks at 30 cm depth to 6 months at 120 cm depth. A preliminary estimate of 3 years was obtained for base flow residence time. These findings all suggest that shallow lateral pathways are not the controlling processes in this tropical forest catchment; rather, the high permeability of soils and substrate lead to vertical rainfall percolation and recharge of deeper layers, and rainfall-runoff responses appeared to be dominated by groundwater discharge from within the hillslope.

Citation: Muñoz-Villers, L. E., and J. J. McDonnell (2012), Runoff generation in a steep, tropical montane cloud forest catchment on permeable volcanic substrate, *Water Resour. Res.*, *48*, W09528, doi:10.1029/2011WR011316.

1. Introduction

[2] The humid tropics are generally remote and largely inaccessible for process-based field studies on streamflow generation. Consequently, the tropical literature has been restricted to a limited number of climatic and landscape combinations, unlike runoff generation literature of the temperate regions (see reviews in *Bonell* [2005] and *Levia et al.* [2011]). A commonly reported feature of tropical forest catchments is their rapid translation of rainfall to runoff via overland flow and shallow subsurface stormflow [*Elsenbeer and Vertessy*, 2000; *Bonell*, 2005], for both the steep montane tropics [*Boy et al.*, 2008; *Goller et al.*, 2005; *Saunders et al.*, 2006; *Schellekens et al.*, 2004] and the lowland tropics [*Bonell and Gilmour*, 1978; *Chappell and Sherlock*, 2005; *Dykes and Thornes*, 2000; *Fritsch*, 1992; *Grimaldi et al.*, 2004; *Elsenbeer and Vertessy*, 2000; *Elsenbeer et al.*, 1995a, 1995b; *Niedzialek and Ogden*, 2010; *Noguchi et al.*, 1997].

[3] While tropical catchment research has covered a reasonably broad geography, steep, tropical montane cloud forest (TMCF) catchments on volcanic substrate have received little or no attention in the literature (see recent review by *Bruijnzeel et al.* [2010] and *Bruijnzeel and Scatena* [2011]). TMCFs are among the world's most valuable terrestrial ecosystems for biodiversity and provisioning of hydrological services to society [*Hamilton et al.*, 1995; *Tognetti et al.*, 2010; *Zadroga*, 1981]. Dramatic degradation and loss of TMCFs worldwide have occurred over the last few decades as a result of high deforestation rates [*Ray et al.*, 2006; *Muñoz-Villers and López-Blanco*, 2008]. Recently, climatic warming and drying related to global or regional climate change have become an important factor that can severely threaten TMCF functioning [*Lawton et al.*, 2001; *Pounds et al.*, 2006].

[4] Notwithstanding the importance of TMCF and their sensitivity to land use and climate change, the states, stocks, flows, and residence times of water cycling in TMCF ecosystems remain very poorly understood. There is therefore a

[1]Department of Forest Engineering, Resources and Management, Oregon State University, Corvallis, Oregon, USA.
[2]Centro de Ciencias de la Atmósfera, Universidad Nacional Autónoma de México, Ciudad Universitaria, Distrito Federal, Mexico.
[3]Global Institute for Water Security, University of Saskatchewan, Saskatoon, Saskatchewan, Canada.

Corresponding author: L. E. Muñoz-Villers, Centro de Ciencias de la Atmósfera, Universidad Nacional Autónoma de México, Circuito Exterior s/n, Ciudad Universitaria, 04510 México, D.F. (lyssette.munoz@atmosfera.unam.mx)

0043-1397/12/2011WR011316

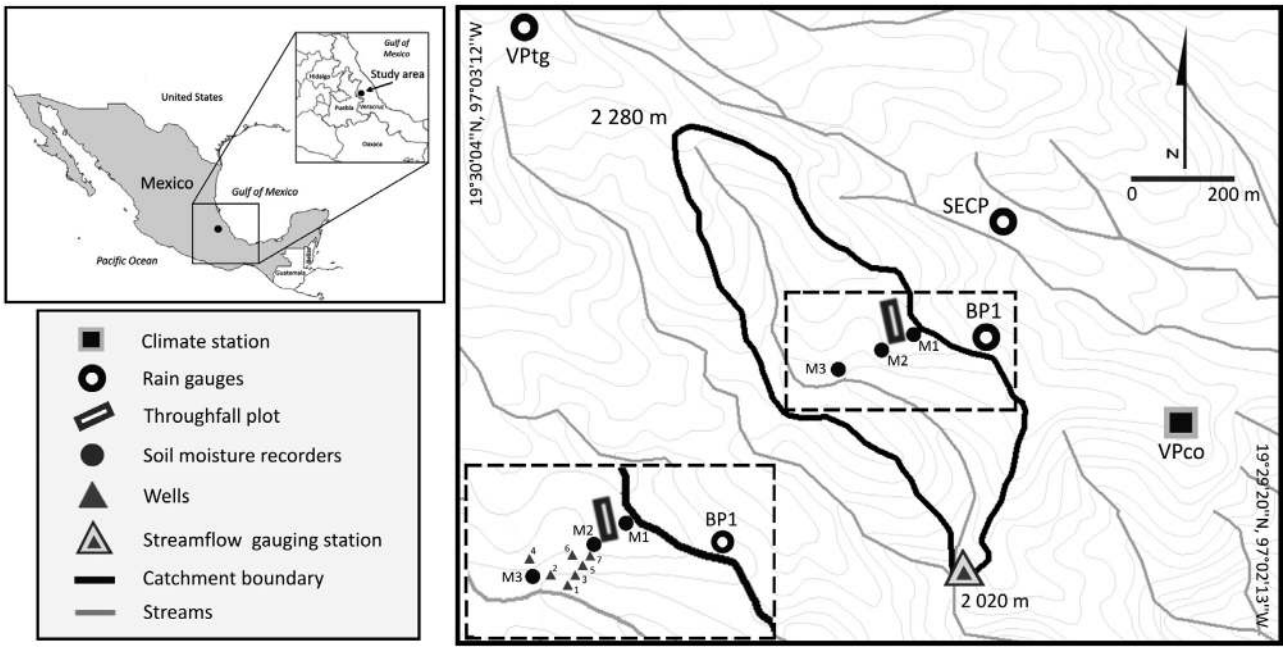

Figure 1. Location of the study area in central Veracruz, Mexico, and map of the old-growth tropical montane cloud forest catchment showing the instrumentation sites. Sources: Topographic data from the Instituto Nacional de Estadística, Geografía e Informática (INEGI, 1993; scale 1:250,000 and INEGI, 2000; scale 1:50,000). Catchment boundary from *Muñoz-Villers* [2008].

pressing need to understand how these ecosystems "work" and to illuminate site-specific information on hydrological functioning for incorporation into conservation and management plans [*Bruijnzeel et al.*, 2010; *Bruijnzeel and Scatena*, 2011]. Unlike other parts of the humid tropics where surface and shallow subsurface flow dominates the storm response to high intensity rainfall, TMCF, particularly on well-drained volcanic substrate, have the potential for deep infiltration and percolation of storm rainfall [*Tobón et al.*, 2010]. However, so little is known about rainfall-runoff processes of these systems that hydrological modeling studies lack basic understanding of how rainfall is partitioned and transmitted to the streams during events. Studies are therefore needed to understand these mechanisms and also the linkages between different spatial scales (plot, hillslope, and catchment) by integrating hydrometric tracer approaches and mean residence time analysis, following important recent work elsewhere in the humid tropics by *Roa-García and Weiler* [2010].

[5] Here we report on the integrated, multiscale rainfall-runoff response of a steep, wet TMCF catchment. Our site is located on the eastern slopes of the Sierra Madre Oriental, which in turn, belongs to the Trans-Mexican volcanic belt [*Geissert*, 1999]. Such volcanic landscapes and their associated soils and geology are widespread around the world; approximately 60% of the world's volcanic ash soils are located in tropical countries [*Takahashi and Shoji*, 2002]. Previous work carried out at this site has suggested that subsurface water mechanisms could be a key factor modulating the catchment runoff hydrology based on the observed high soil porosities and hydraulic conductivities and annual total streamflow consisting largely of base flow [*Karlsen*, 2010; *Marín-Castro*, 2010; *Muñoz-Villers et al.*, 2012]. To understand the hydrological functioning and dominant processes contributing to stream runoff generation in this tropical montane forest system, we used a combination of hydrometric-tracer field observations at different spatial and temporal scales over a period of increasing antecedent wetness (wetting-up cycle) during the 2009 wet season and water transit times. We addressed the following specific research questions:

[6] 1. Does overland flow and shallow subsurface storm-flow control hillslope and catchment response as observed in other areas of the humid tropics?

[7] 2. Are flow sources and pathways consistent through the wetting-up cycle?

[8] 3. What are the characteristic mean residence times of soil water and stream base flow?

2. Site Description

[9] The research was carried out in a headwater montane cloud forest catchment (24.6 ha) located between 2020 and 2280 m a.s.l. on the eastern slopes of Cofre de Perote volcano (19°29′34″ N, 97°02′42″ W); part of the catchment belongs to the La Cortadura Forest Reserve of the municipality of Coatepec, Veracruz State (central eastern Mexico; Figure 1). The catchment has steep (20 to 40°, covering 52% of the area [*Muñoz-Villers*, 2008]) and short (<250 m) slopes with deeply incised valleys, drained by a first-order perennial stream. The type of soil is Umbric Andosols derived from volcanic ash [*Campos*, 2010]. In the middle and upper portion of the hillslopes, soil profiles are multilayered (A A/B, Bw, Bw/C, and C) ranging from 1.5 to 3 m depth, whereas the near-stream areas are characterized by much shallower (from 0.5 to 1 m) and less developed soils (A, BW, and C) [*Marín-Castro*, 2010]. The soils are strongly acidic (pH ∼ 3.5

[*Campos*, 2010]) and composed on average of 44% silt, 21% sand, and 34% clay [*Marín-Castro*, 2010]. A general description of the soil profile along the hillslope showed a black to very dark brown, loam, organic, granular A horizon (0–20 cm) overlying a dark yellowish brown, loam slightly clayey, medium granular B horizon (20–80 cm), followed by a reddish brown, silt clay loam, subangular blocky C horizon (80–300 cm) [*Marín-Castro*, 2010]. The soils are mostly covered by a litter layer of *Quercus* sp., with a thickness of about 10 cm [*Muñoz-Villers*, 2008]. Topsoils (1–10 cm) are characterized by low bulk densities (0.26 g/cm^{3}on average), high porosities (79%), high organic matter content (50% of organic carbon), and very high saturated hydraulic conductivities (*Kfs*)(777 ± 931 (SD) mm/h [*Marín-Castro*, 2010; *Muñoz-Villers et al.*, 2012]). The underlying soil layers showed bulk densities that increased from 0.36 g/cm^3 (B horizon) to 0.76 g/cm^3 (C horizon), whereas porosities and soil organic carbon decreased from 77 to 62% and 21 to 5%, respectively. Saturated hydraulic conductivities along a 1.5 m soil profile showed that *Kfs* decreases with depth (from about 1000 mm/h at 10 cm to about 4 mm/h at 150 cm [*Karlsen*, 2010]). Residual water retentions ranged from 0.04 and 0.12 cm^3/cm^3 across all soil horizons [*Geris*, 2007].

[10] The soils are underlain by permeable, moderately weathered andesitic volcanic breccias underlain, in turn, by permeable saprolite that has been weathered from fractured andesitic-basaltic rock. The depth to bedrock ranged approximately from 4 m in the near-stream areas to more than 10 m on the hilltops, as estimated using borehole logs from wells (see Figure 1; L.E. Muñoz-Villers and C. Gabrielli, unpublished data, 2010) and geoelectrical soundings over the hillslopes [*Karlsen*, 2010]. Estimates of bedrock permeability to deep groundwater are ∼1.9 mm/day [*Muñoz-Villers et al.*, 2012].

[11] The climate in the study area is classified as temperate humid with abundant rains during the summer [*Garcia*, 1988]. Two distinct seasons can be distinguished: (1) a wet season (May–October), during which rainfall is associated primarily with cumulus and cumulonimbus clouds formed during convective and orographic uplift of the moist maritime air masses brought in by the easterly trade winds; and (2) a (relatively) dry season (November–April), during which most rainfall falls from stratus clouds associated with the passage of cold fronts [*Báez et al.*, 1997]. Total annual rainfall is about 3200 mm, of which typically 80% falls during the wet season [*Holwerda et al.*, 2010; *Muñoz-Villers et al.*, 2012]. Fog interception occurred exclusively during the dry season and accounted for ≤2% of the annual rainfall [*Holwerda et al.*, 2010]. The average annual temperature measured at a climate station located at 320 m of our catchment (VPco; Figure 1) is 14.4°C [*Holwerda et al.*, 2010] and the mean annual reference evapotranspiration ET_0 as calculated using data from the same weather station is 855 mm [*Muñoz-Villers et al.*, 2012].

[12] The forest is an old-growth lower montane cloud forest and represents a unique biodiversity refuge of the central part of Veracruz [*García-Franco et al.*, 2008; *Castillo-Campos et al.*, 2009]. The forest is characterized by a dense canopy cover, with an average Leaf Area Index of 6.3 m^2/m^2 (M. Gómez-Cárdenas, unpublished data, 2010). The average tree height is 27 m and the average diameter of the trees at breast height (*dbh*) is 0.3 m [*García-Franco et al.*, 2008]. The most common tree species in the overstory are *Quercus corrugata*, *Clethra macrophylla*, *Parathesis melanosticta*, and *Alchornea latifolia.* The forest is also rich in vascular epiphytic species [*García-Franco et al.*, 2008].

3. Methods

3.1. Hydrometeorological Measurements

[13] Due to the lack of sufficiently large clearings in the forest and difficulties obtaining site permissions in privately owned areas, rainfall (*P*) was measured at only one site in the catchment (Figure 1). Additional rain gauges were installed at the weather station (VPco) and in open areas to the east (SECP) and north (TG1) of the catchment (Figure 1). The rain gauges were of the type ARG100 (Environmental Measurements Ltd.), Casella CEL, and RG2M (Onset) (all with a resolution of 0.2 mm). For additional details on the logger systems, refer to *Muñoz-Villers et al.* [2012]. All gauges were dynamically calibrated to account for the variable error associated with the loss of water during bucket rotation [*Calder and Kidd*, 1978]. Continuous measurements of rainfall were made between November 2008 and October 2010.

[14] Streamflow (*Q*) was measured using 90° V notch weir installed at the catchment outlet (Figure 1). Water levels were measured every 2 min using Schlumberger LT F15/M5 pressure transducer paired with F5/M1.5 Baro-Divers to compensate for atmospheric pressure (see *Muñoz-Villers et al.* [2012] for further details on instrumentation and calibration procedures). Streamflow measurements were available from November 2008 to June 2010.

[15] Soil volumetric water content (VWC) was measured every 10 min using capacitance-based sensors (type 10 HS) connected to an EM50 data logger (Decagon Devices Inc., USA) from April 2009 to October 2010. Measurements were made at three different positions along a south-facing hillslope transect (ridge top (M1), midslope (M2), and near-stream valley bottom (M3); Figure 1). The instrumented hillslope was 250 m long, with an average slope of 30°. At each position, five soil moisture probes were installed horizontally at different depths (8, 20, 40, 65, and 95 cm on average) according to the array of horizons observed in the first 1.5 m of soil. When the observation period concluded, each VWC probe was calibrated at the Soil Laboratory of the Instituto de Ecología A.C., Xalapa, Veracruz using undisturbed soil cores with a diameter of 10.4 cm and a length of 20 cm extracted from the field using PVC tubes (E. Hincapié *et al.*, manuscript in preparation, 2012). The calibration followed the standard procedure for calibrating capacitance sensors outlined by *Starr and Palineanu* [2002].

[16] Groundwater levels were measured using a network of seven wells located in the lower portion of the hillslope (Figure 1). The wells ranged in depth between 5.3 and 10.8 m, where W1 and W4 were the shallowest and the deepest, respectively. Depths of the other wells were W2 = 8.4 m; W3 = 6.7 m; W5 = 9.0 m; W6 = 9.0 m; and W7 = 10.0 m. All wells were drilled into the bedrock following the method of *Gabrielli and McDonnell* [2011] and cased using 5 cm diameter PVC tubes that were screened with 3 mm horizontal slots from 10 cm below the soil-breccia interface to their completion depths in the permeable weathered breccias-saprolite. Further, the wells were sealed with bentonite at the

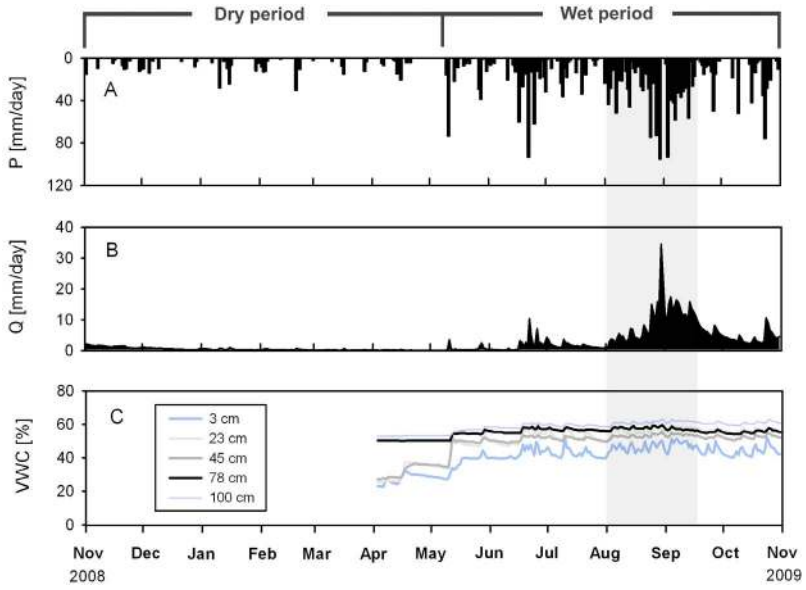

Figure 2. (a) Daily totals of rainfall (P) as measured at the mature TMCF catchment between November 2008 and November 2009 and corresponding average daily values of (b) streamflow (Q) and (c) volumetric water content (VWC, %) for 5 soil depths at the ridge top location (M1, Figure 1). The gray shaded area indicates the wetting-up cycle of the 2009 wet season.

ground level to prevent surface water infiltration into them. Water level in Well 1 was measured every 5 min using a Schlumberger LT F15/M5 pressure transducer paired with a F5/M1.5 Baro-Diver for atmospheric pressure measurement. Water heights in Wells 2 to 7 were measured manually at weekly intervals during the 2009 wet season.

3.2. Isotope Sampling

3.2.1. Rainfall-Runoff Event Sampling

[17] The hydrological response of the catchment to rainfall events was examined during a period of increasing antecedent wetness (wetting-up cycle) that occurred from 1 August 2009 and lasted approximately 6 weeks until mid-September (Figure 2). During this period, samples of rainfall, throughfall, and stream water were intensively collected on a storm event basis for stable isotope (δ^2H and δ^{18}O) analysis. Measurements of electrical conductivity (EC) were carried out in situ for each water sample collected for isotopes using a portable EC meter (Oakton, Model 300 Series). Previous studies have successfully used EC along with conservative tracers to differentiate the spatial sources of water within catchments [*McDonnell et al.*, 1991a, 1991b; *Laudon and Slaymaker*, 1997; *Stewart et al.*, 2007; *Jencso et al.*, 2010].

[18] A storm was defined as a period with more than 0.2 mm of rainfall, separated by a dry period of at least 3 h [cf. *Gash*, 1979; *Cuartas et al.*, 2007; *Holwerda et al.*, 2010]. Since wet season rainfall in this area is primarily of convective origin [*Báez et al.*, 1997], this type of rain-producing system was mainly targeted for the rainfall-runoff sampling. Rainfall was collected in 5 mm increments using a passive sequential sampler [*Kennedy et al.*, 1979]. The sequential rain sampler was paired with a tipping bucket rain gauge (SECP; Figure 1). At the same location, bulk samples of rainfall were collected using a rainwater sampler consisting of a 9.5 cm diameter funnel assembled to a 4 cm diameter and 40 cm long transparent collection tube. The tube contained a float to minimize evaporation. The rain gauge was inserted in 7.5 cm diameter PVC pipe wrapped by bubble foil insulation to protect the collected water against direct sunlight and minimize temperature variations. The PVC tube was partly buried so that the opening of the funnel was at about 30 cm above the ground.

[19] No attempt was made to collect sequential samples of throughfall because of the difficulties involved in getting a representative sample due to the large spatial variability of throughfall in tropical forests [e.g., *Holwerda et al.*, 2006]. However, bulk samples of throughfall were collected for comparison with rainfall. Throughfall samples were obtained using 10 collectors distributed randomly along the instrumented hillslope. The collectors consisted of 7.5 cm diameter plastic funnel draining into a 500 ml plastic water bottle. The water bottle was again inserted in 7.5 cm diameter PVC pipe to protect the sample against solar radiation.

[20] Stream water was collected during the storms using an automatic water sampler (Model 3700C, Teledyne ISCO, Inc., USA) installed at the streamflow gauging station (Figure 1). The stream sampler was programmed to start sampling 1 to 2 h before the storm was expected to start (to include at least one sample of pre-event base flow) and to take samples at constant intervals (30, 40, and 60 min). The sampling frequency was increased progressively through each event because the stream hydrograph recessions became longer as catchment wetness increased. In addition, base flow samples were manually collected on a weekly basis.

[21] Soil water was collected from porous cup lysimeters (Soil Moisture Equipment, Corp., USA) using a suction of about 60 kPa prior to each storm sampling. The lysimeters were installed at a maximum distance of 2 m from the soil moisture sensors. At the ridge top (M1) and midslope (M2) positions (Figure 1), four lysimeters were installed at 30, 60, 90, and 120 cm depth, whereas in the near-stream valley (M3),

where the soils are much shallower, only three lysimeters were installed at 30, 60, and 90 cm depth. For comparison with prestorm stream base flow, a few samples of groundwater were taken during the second half of the sampling period from the wells located near the stream (Wells 1 and 2), since these were the ones that showed a permanent water table throughout the wet period. The wells were pumped dry and allowed to recharge before a sample was taken.

3.2.2. Rain, Soil, and Stream Base Flow Sampling for Transit Time Estimates

[22] Over the course of 2 years (2008 to 2010), samples of soil water from lysimeters at low suction (60 kpa) and stream base flow during nonstorm conditions and rainfall were collected for δ^2H and δ^{18}O analysis. Bulk samples of rainfall were collected at SECP from 14 November 2008 to 29 October 2010. The sampling intervals ranged between 1 and 25 days, with a frequency of 3 and 13 days (on average) for the wet and dry seasons, respectively. Between 14 November 2008 and 29 October 2010, grab samples of base flow were collected every 2 weeks at the stream gauging station. From 5 August 2009 to 14 May 2010, soil water samples were collected every week at different depths (30, 60, 90, and 120 cm) and across various hillslope positions (ridge, midslope, and downslope).

3.2.3. Isotope Collection and Analysis

[23] Water samples for isotope analysis were collected in 30 ml borosilicate glass vials with polycone sealing cap to prevent evaporation. The samples were analyzed for δ^2H and δ^{18}O on a laser liquid-water isotope spectrometer (Version 2, Los Gatos Research, Inc.) at the Hillslope and Watershed Hydrology Lab at Oregon State University, USA. The isotope values are expressed in permil (‰) relative to Vienna Standard Mean Ocean Water (VSMOW). The precision of the δ^2H and δ^{18}O measurements was 0.3 and 0.1‰, respectively.

3.3. Hydrograph Separation Techniques

[24] Antecedent precipitation index (*API*) was calculated for each storm to determine the antecedent moisture conditions for the 7 and 15 days prior to those storms, according to *Viessman et al.* [1989]. Streamflow was separated into base flow (Q_b) and quickflow (Q_d) using the method of *Hewlett and Hibbert* [1967]. The separation was performed using a slope constant of 0.030 mm/h [*Muñoz-Villers et al.*, 2012]. A one-tracer, two-component separation [*Pinder and Jones*, 1969; *Sklash and Farvolden*, 1979] was conducted to partition storm runoff into its pre-event (water stored in the catchment prior to the event) and event (water input to the catchment) water sources using the following mixing equation:

$$Q_t C_t = Q_p C_p + Q_e C_e \tag{1}$$

where Q_t, Q_p, and Q_e represent current streamflow, pre-event, and event water volumes, respectively, and C_t, C_p, and C_e are the corresponding δ^2H or δ^{18}O isotope concentrations. The average of the tracer concentrations of the base flow samples taken within the 2 h prior to the storm was taken as representative of C_p [*Sklash and Farvolden*, 1979]. C_e at a specific time was determined as the incremental weighted mean of the isotopic composition of the rainfall up to that time [*McDonnell et al.*, 1990].

[25] Further, a two-tracer three component separation [*Ogunkoya and Jenkins*, 1993] was carried out to examine the contributions of soil water and groundwater (both components of pre-event water) to streamflow using δ^2H or δ^{18}O isotope ratios and EC as follows:

$$Q_t C_t = Q_e C_e + Q_s C_s + Q_g C_g \tag{2}$$

where Q_t, Q_e, Q_s, and Q_g are the assumed components of total storm runoff (current streamflow, event, soil, and groundwater volumes, respectively), and C_t, C_e, C_s, and C_g are the corresponding tracer concentrations. C_s was calculated as the average value of the tracer concentrations across soil depths and topographic positions in the catchment. Because of the logistical difficulties involved in taking samples of groundwater from the wells before each storm, C_g was assumed equal to the average tracer concentration of base flow measured prior to the storm (i.e., C_p). A comparison between the isotopic composition of prestorm base flow and groundwater showed no statistical differences (see section 4.2.2). The uncertainty associated in the calculation of the pre-event fractions was quantified using the error propagation technique of *Genereux* [1998] at the 0.05 confidence level.

3.4. Transit Time Model

[26] Weekly and biweekly δ^2H and δ^{18}O signals of soil and stream water were used to estimate their mean transit times (MTT) and transit time distributions (TTD). While the δ^2H and δ^{18}O precipitation data collected over 2 hydrological years (November 2008 to October 2010) may be too short to properly constrain stream base flow MTT estimates [cf. *Hrachowitz et al.*, 2009], precipitation variations at our site showed a marked seasonal pattern [*Holwerda et al.*, 2010; *Muñoz-Villers et al.*, 2012]. Rainfall isotope signatures also showed a strong and consistent variation with rainfall amount [*Goldsmith et al.*, 2012]. To generate a warm-up period required for the model simulations, we repeated our measured 2-year rainfall time series 15 times following the approach of *Hrachowitz et al.* [2009, 2010]. We then used a lumped parameter convolution model to predict both δ^2H and δ^{18}O outputs for the soil and stream water as a weighted sum of their respective past δ^2H and δ^{18}O measured inputs in precipitation [*Stewart and McDonnell*, 1991; *Maloszewski and Zuber*, 1993]. Mathematically, the soil or stream water outflow composition at any time, $\delta_{out}(t)$, consisted of past inputs lagged, $\delta_{in}(t\text{-}\tau)$, weighted by the transfer function $g(\tau)$ which represents its lumped transit time distribution (TTD) [*Maloszewski and Zuber*, 1982]:

$$\delta_{out}(t) = \int_0^\infty g(\tau)\delta_{in}(t-\tau)d\tau \tag{3}$$

where τ are the lagged times between the input and output tracer composition. The weighting function or transit time distribution (TTD) describes the travel time of the water from the ground surface to an outflow location (i.e., soil water or catchment stream water)[*McGuire and McDonnell*, 2006, 2010].

[27] Equation (3) considers only the rainfall input concentrations of the conservative tracer. However, it is the actual input tracer mass flux (or input mass weighted concentration) that determines the mixing and the resulting output concentration δ_{out}. Thus the input concentration was

biweekly and weekly mean volume weighted $w(t - \tau)$ adjusted for recharge to predict streamflow and soil water outputs at these time steps:

$$\delta_{out}(t) = \frac{\int_0^\infty g(\tau)w(t-\tau)\delta_{in}(t-\tau)d\tau}{\int_0^\infty g(\tau)w(t-\tau)d\tau} \quad (4)$$

where a recharge fraction of 0.9 was used to account for rainfall interception losses derived from *Holwerda et al.* [2010].

[28] Examples of common TTD used include the exponential, exponential-piston flow and dispersion model [*Maloszewski and Zuber*, 1982; *Kreft and Zuber*, 1978], the gamma distribution [*Kirchner et al.*, 2001] and the two parallel lineal reservoir model (TPLR) [*Weiler et al.*, 2003]. We evaluated each of these TTD functions using the transfer function hydrograph separation model TRANSEP [*Lyon et al.*, 2008; *McGuire and McDonnell*, 2010; *Roa-García and Weiler*, 2010; *Weiler et al.*, 2003]. TRANSEP helps to identify which of these distributions will provide the best goodness of fit to the observed δ^2H and δ^{18}O outputs (i.e., soil and stream water) (refer to *McGuire and McDonnell* [2006] for further details). TRANSEP utilizes the Generalized Likelihood Uncertainty Estimation (GLUE) methodology [*Freer et al.*, 1996] based on Monte Carlo simulations to determine the identifiability of the individual parameters. Our Monte Carlo analysis of each TTD consisted of 10,000 runs. The criterion used to assess model performance was the Nash–Sutcliffe efficiency E [*Nash and Sutcliffe*, 1970], based on the best agreement parameter value, where a value of 1 would indicate a perfect fit. Parameter uncertainty was defined as the range between 0.1 and 0.9 percentile parameter value for the best 20% performing parameter sets based on E [*McGuire and McDonnell*, 2010; *Seibert and McDonnell*, 2010]. The overall performance of the TTD models (either soil or stream water) was evaluated using the root mean square error (RMSE).

4. Results

4.1. General Hydrometeorological Conditions

[29] During the 2008/2009 hydrological year (1 November to 31 October), total rainfall (P) was 2975 mm, of which about 86% fell during the wet season (May–October) (Figure 2). Mean monthly P during the wet season (424 mm) was almost six times that observed during the dry season (72 mm). Highest monthly P amounts were recorded in August and September and lowest during the months of March and April.

[30] Total annual streamflow (Q) was 885 mm (30% of P) and consisted largely of base flow (87% of total Q). The mean monthly Q during the wet season (132 mm) was almost nine times higher than that during the dry season (15 mm). Streamflow observed during the wet season accounted for 90% of the total annual Q. From the total of 200 rainfall events, 145 rain events occurred during the rainy season, and 87 of those produced runoff during rainfall (quickflow; Q_d). Q_d volumes were largely, if not at all, generated during the rainy season; wet season Q_d accounted for 4% and 14% of the total annual P and Q, respectively. Q during the dry season consisted almost entirely of base flow (Q_d/Q = 1% and Q_d/P < 1%).

[31] Since the soil volumetric water content (VWC) measurements were initiated at the end of the dry season (April 2009), the values reported below as dry season values may be biased low. The mean daily soil moisture across all soil depths and topographic locations was 57.9 ± 7.9% on average for the wet season (range: 27–78%) and 48.4 ± 11.8% for the dry season (range: 23–69%). The soils showed lower mean moisture contents at the shallower depths compared to the deeper layers during both the dry and wet seasons (Figure 2). Overall, the highest soil moisture values were reported at the near-stream location (M3: 65 ± 6%; range: 52–78%) and the lowest values at the upslope position (M1: 51 ± 9%; range: 23–63%), meanwhile the midslope location showed intermediate values (M2: 58 ± 5%; range: 43–67%). Maximum mean daily VWC values were recorded in the months of August and September (M1:63%, M2:66%; and M3:76%) when antecedent precipitation amounts and streamflow discharge were also highest (Figure 2).

4.2. The 2009 Wetting-Up Cycle

[32] The 2009 wet season experienced an anomalous 1-month dry spell (from 2 to 31 July), which was associated to an El Niño-Southern Oscilation (ENSO) event that affected most of the Mexican territory (http://smn.cna.gob.mx). As a result, on a national scale, July 2009 was registered as the second driest July since 1941 [*SMN*, 2009a, 2009b]. The rainfall recorded in July at La Cortadura (214 mm) was only 48% of the average July rainfall measured since 2005 (450 mm).

[33] Total P during the 6-week wetting-up cycle starting at the beginning of August was 1203 mm (47% of the total wet season P), distributed in 47 discrete rainfall events. Median storm size (event P distribution positively skewed) and duration were 21.7 mm (range: 0.4–100 mm) and 4 h (range: 2–12 h), respectively. The median rainfall intensity was 3.5 mm/h (range: 0.2–61 mm/h). The average time between storms was 19 ± 11 h (range: 4–56 h), indicating that there was typically one event per day. Rain events occurred predominately during the end of the afternoon and early evening in the form of orographic-convective storms.

[34] Streamflow response to this type of storm was typically in the form of a single-peak hydrograph with a sharp rising limb and slow recession. At the start of the wetting-up cycle, Q_d/P and Q/P event ratios were only a small fraction of the rainfall (0.05 and 0.07 on average, respectively; Figure 3), but as antecedent soil moisture and rainfall amounts increased, Q_d/P and Q/P ratios increased up to an mean maximum of about 0.08 and 0.40, respectively.

4.2.1. Hillslope and Catchment Event Responses

[35] A total of 13 rainfall events with depths between 15 and 110 mm were sampled for hydrograph separation analysis during the 2009 wetting-up cycle, with antecedent wetness conditions ranging from relatively dry (API_7 = 9 mm; API_{15} = 66 mm) to very wet (API_7 = 284 mm; API_{15} = 460 mm). From these 13 storms, seven were discarded because (1) the stormflow sampling did not cover the entire stream hydrograph (two storms); (2) storms of less than 20 mm did not produce a significant increase in the streamflow (two storms); (3) the difference between the isotope composition of rainfall and pre-event stream water was not enough to perform hydrograph separation analysis (three

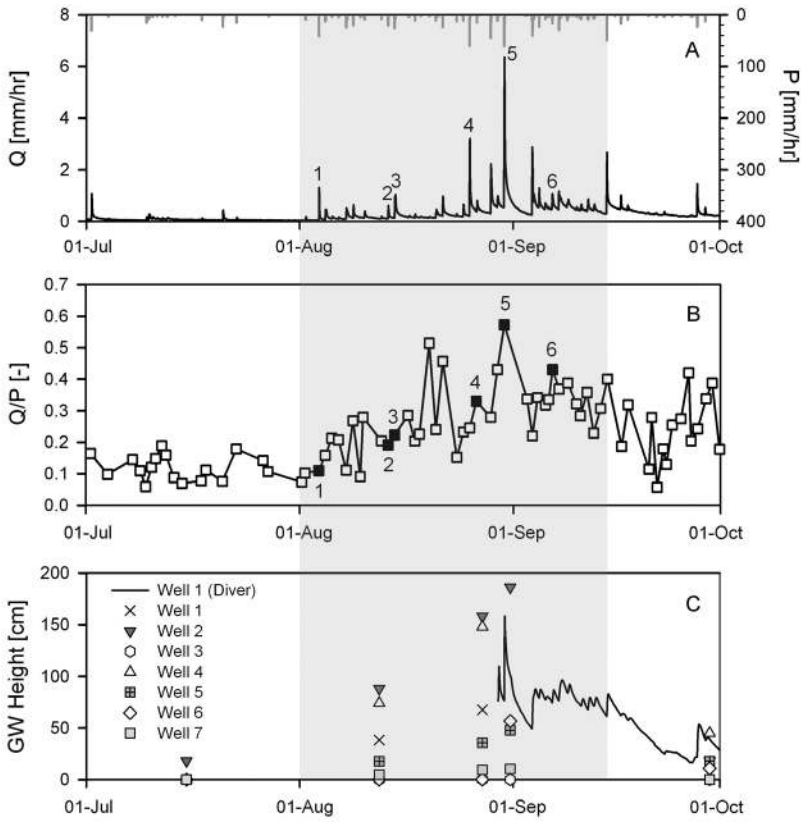

Figure 3. (a) Hourly values of rainfall (P) and streamflow (Q) as measured at the TMCF catchment from July to October 2009 and (b) the corresponding storm runoff ratios (Q/P). The numbers in Figures 3a and 3b denote the six rain storms analyzed using the various hydrograph separation techniques (see text). (c) Readings of groundwater levels for the seven wells installed in the investigated hillslope (symbols). The line shows hourly values of groundwater height for Well 1 as measured from 31 August to 1 October 2009. The gray shaded area indicates the wetting-up cycle of the 2009 wet season.

storms). Therefore a total of six storms were analyzed (Figure 3a). The event characteristics of these six storms are summarized in Table 1. Rainfall depths and maximum intensities of these events ranged between 23 and 101 mm and from 16 to 63 mm/h, respectively. The highest rainfall intensities were registered for convective storms enhanced by the instability associated with the tropical waves (Storms 1 and 5; Table 1). Rainfall durations were between 2 and 9 h. Q_d/P and Q/P ratios ranged from 0.05 to 0.23 and 0.11 to 0.54, respectively, and increased progressively from Storm 1 to Storm 6 as antecedent wetness also increased (Figure 3b). The maximum water yield was produced by Storm 5, which occurred at the height of the wetting-up cycle and was the largest and most intense event of the 2009 wet season (101 mm in 4 h).

Table 1. Summary of the Rainfall and Storm Runoff Characteristics of the Six Storms Analyzed During the Wetting-Up Cycle of the 2009 Wet Season

	Storm 1	Storm 2	Storm 3	Storm 4	Storm 5	Storm 6
Date	3 Aug 2009	13 Aug 2009	14 Aug 2009	26 Aug 2009	30 Aug 2009	6 Sep 2009
Rain producing system	Tropical wave 19	Convection	Convection	Convection	Tropical wave 27	Convection
P total, mm	35	23	44	31	101	34
Mean *I*, mm/h	17	12	11	3	25	8
Maximum *I*, mm/h	33	16	23	20	63	18
Rainfall duration, h	2	2	4	9	4	4
Q_d, mm	1.7	0.8	3.2	0.85	22.8	2.6
Q, mm	3.8	4.5	10.2	10.1	54.4	14.6
Q_d/P	0.05	0.04	0.07	0.03	0.23	0.08
Q/P	0.11	0.20	0.23	0.33	0.54	0.43
Peak discharge, mm/h	1.3	0.6	1.0	0.8	6.4	1.0
Time lag, min	40	50	80	80	40	70
Time to peak discharge, min	70	80	100	120	70	120
7 day *API*, mm	9	142	134	162	185	284
15 day *API*, mm	66	208	219	274	311	460

Table 2. Mean ± Standard Deviation, Minimum and Maximum Values of the Isotope Ratios (δ^2H and δ^{18}O) and EC Concentrations of Rainfall, Soil and Groundwater, Base Flow, and Stream Water Corresponding to the Six Storm Events Analyzed Using Hydrograph Separation Techniques[a]

		δ^2H, ‰			δ^{18}O, ‰			EC, μS/cm		
		Mean ± SD	Min	Max	Mean ± SD	Min	Max	Mean ± SD	Min	Max
Bulk rainfall	(n = 6)	−29.8 ± 24.4	−76.6	−10.3	−5.7 ± 3.1	−11.6	−2.7	8.9 ± 3.7	3.4	14.2
Rainfall[b]	(n = 6)	−28.8 ± 21.2	−68.5	−9.7	−5.5 ± 2.7	−10.5	−2.9	6.7 ± 2.2	3.6	9.5
Soil water[c]	(n = 65)	−38.6 ± 3.5	−42.5	−32.5	−6.7 ± 0.5	−7.3	−5.9	31.0 ± 3.7	27.5	37.0
Stream water[d]	(n = 131)	−40.0 ± 3.6	−46.1	−29.5	−6.9 ± 0.5	−7.7	−5.3	15.8 ± 2.9	12.6	26.4
Base flow[e]	(n = 17)	−43.2 ± 0.8	−44.4	−42.3	−7.4 ± 0.3	−7.8	−7.1	14.9 ± 1.0	13.9	16.4
Groundwater	(n = 4)	−44.6 ± 2.3	−47.2	−43.2	−7.7 ± 0.2	−7.8	−7.5	-	-	-

[a]Here n = total number of samples.
[b]Average of volume-weighted mean values of rainfall collected with the sequential rain sampler. Each storm consisted of eight discrete samples of rain on average.
[c]Average value across all locations and depths (11 samples on average per storm).
[d]Average of the stream water samples collected during rainfall (22 samples on average per storm).
[e]Average of base flow samples collected within the 2 h prior to the storm runoff sampling (three samples on average per storm).

[36] Stream and soil moisture response to these 6 rain events was analyzed using the 10-min data. Lag times between peak rainfall and peak discharge ranged from 40 to 80 min. Time to peak discharge ranged between 70 and 120 min (Table 1). Lag time and time to peak were related to both rainfall event characteristics and catchment wetness conditions (Table 1).

[37] From the start to the end of the 6-week wetting-up cycle, the average soil moisture content across all locations showed a small increase of about 5% in both the shallower (0–50 cm: from 55 to 60%) and deeper soil layers (50–100 cm: from 58 to 63%). Soil moisture response to peak rainfall was lagged, and time lags became longer with soil depth and increasing antecedent wetness. The near-surface soil layer (A horizon) generally responded faster than streamflow, whereas the deeper soil layers (Bw/C horizons) were slower to react. The highest variation in soil moisture was observed in the near-surface layers (particularly at upslope position, M1), whereas the deeper soil layers showed the smallest changes (specifically at the downslope position, M3). Although the downslope site registered very high values of soil moisture, none of the VWC probes reached the saturation level, suggesting that perched water tables were not formed. Maximum VWC response to rainfall overall was observed for Storms 1 and 5. The shallower soil depths responded quickly to these events (∼20 min) and increased beyond their prestorm soil moisture content by +20 and +30%, for Storms 1 and 5, respectively. Deeper soil layers on the other hand showed much smaller increases in VWC (5% on average), and their time lag response varied significantly between Storms 1 and 5 (∼330 min versus 70 min, respectively) likely due to differences in their antecedent soil moisture conditions.

[38] Event-based data for groundwater response to rainfall was not available for all the wells. Nevertheless, some qualitative observations of hillslope groundwater can be made from the available information. Water tables were first detected in the near-stream valley area (W1 and W2) after antecedent precipitation had increased from 42 to 90 mm (first week of the wetting-up cycle). As wetness conditions increased, the other hillslope wells gradually developed water tables (Figure 3c). Wells W1, W2, and W4 showed the highest and most persistent water levels throughout the study period. Conversely, water tables in wells W5, W6, and W7 were highly transient and only occurred during periods with consecutive and heavy rainstorms. Well W3 remained dry for the entire period. The maximum rise in groundwater was observed for Storm 5. The hillslope showed a temporary hydrological connectivity between wells for this storm, triggered by the high rainfall amount and intensity, along with the high antecedent wetness status of the catchment. The 10-min water level data collected in well W1 during the second half of the study period showed a strong logarithmic relation (r^2 = 0.89) with the streamflow, suggesting hydrological connectivity between the riparian groundwater and the stream catchment outlet.

4.2.2. Isotope and EC End-Members Signatures

[39] The variation of volume-weighted mean δ^2H and δ^{18}O values was greatest for rainfall (from −68.5to −9.7‰ for δ^2H and from −10.5 to −2.9‰ for δ^{18}O) and smallest for stream base flow (from −44.4 to −42.3‰ for δ^2H and from −7.8 to −7.1‰ for δ^{18}O; Table 2). A distinct difference was observed between the isotope ratio of storms produced by "regular" convective-orographic uplift (Storms 2 to 4) and those associated with tropical wave systems (Storms 1 and 5); the latter were more negative (i.e., lighter composition) as compared to the former, with a mean difference of −34.1‰ and −4.2‰ for δ^2H and δ^{18}O, respectively. The lowest δ^2H and δ^{18}O values in rainfall and runoff were associated with Storm 5, which was produced by tropical wave 27 during the rainiest period of the wet season (Figure 4). Throughfall in general showed the most positive isotope ratios (i.e., heaviest) of all end-members; however, the difference found between throughfall and rainfall was small (+1.13‰ and +0.01‰ for δ^2H and δ^{18}O, on average) and not significant at 0.05 level (p = 0.903 and p = 0.976, respectively).

[40] The δ^2H and δ^{18}O values in storm runoff showed a progressive variance decrease from Storm 1 to Storm 6 and converged to the mean annual base flow values (−42.1‰ and −7.3‰ for δ^2H and δ^{18}O, respectively) when antecedent precipitation was the highest. Soil water showed values of δ^2H and δ^{18}O intermediate to those of rainfall and stream base flow. The average isotope ratio of groundwater (44.6‰ and −7.7‰ for δ^2H and δ^{18}O, respectively) was not significantly different from that of base flow (−43.2‰ and −7.4‰; p = 0.207 and p = 0.124, respectively). The EC values of soil water were highest and showed the greatest variation of all end-members. Rainwater showed the lowest concentration of EC and with least variation, followed by throughfall (Table 2).

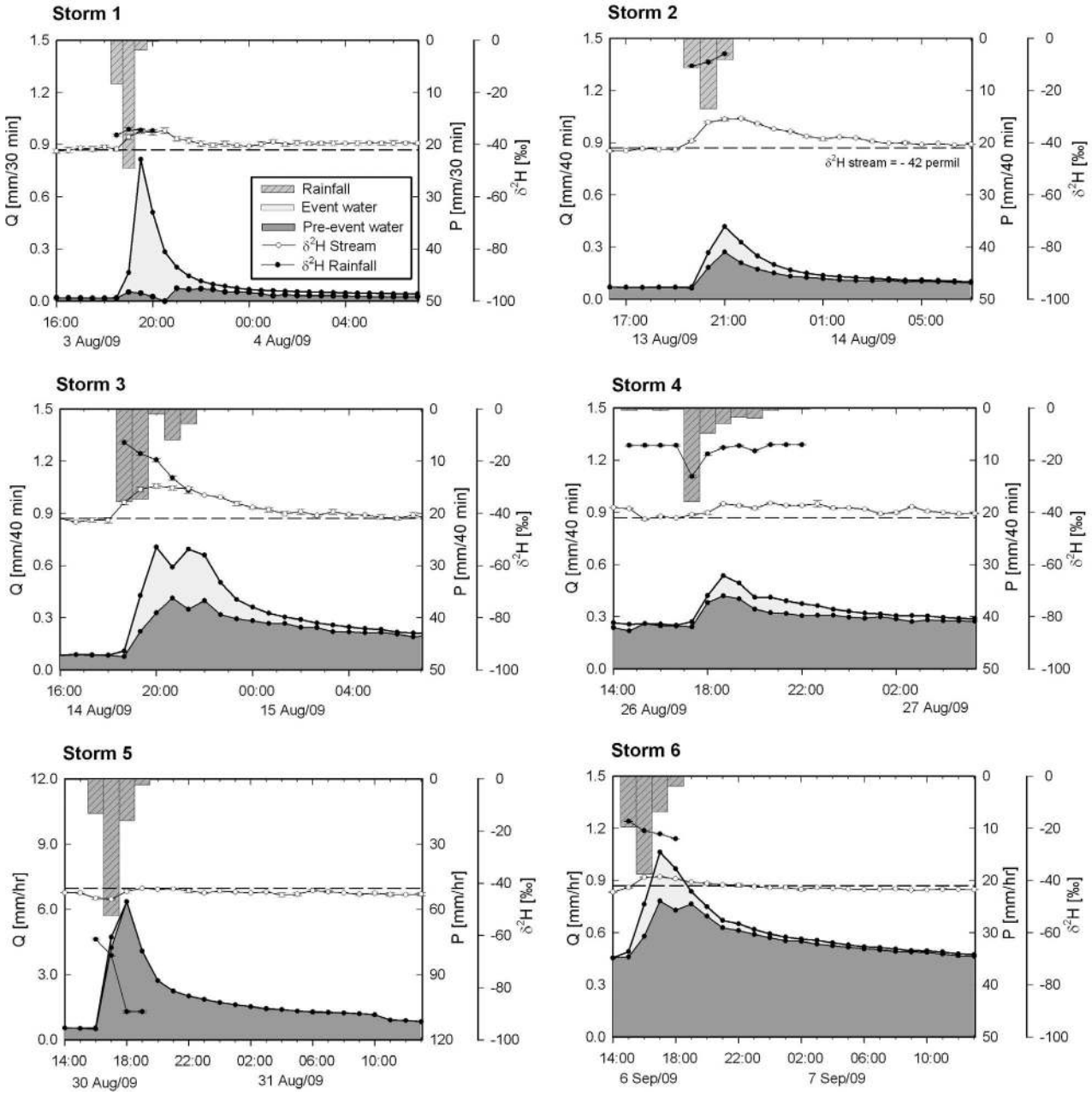

Figure 4. The partitioning of storm runoff into its pre-event and event water sources using one-tracer two component hydrograph separation analysis with δ^2H as tracer for the six rain storms sampled during the wetting-up cycle of the 2009 wet season. The error bars represent the δ^2H analytical precision. Note that the rainfall (P) and streamflow (Q) data for Storm 5 are plotted on different scales for a better representation.

4.2.3. Storm Runoff Sources

[41] The one-tracer two component hydrograph separation analysis (using both δ^2H and δ^{18}O as tracers) showed a clear, progressive increase of the pre-event water contribution to total stormflow through the wetting-up cycle (Figure 4). The first storm had relatively dry antecedent conditions and showed a very low pre-event water percentage (31% and 38% for δ^2H and δ^{18}O, respectively). The last storms in the temporal sequence occurred at very wet antecedent conditions and showed very high pre-event water proportions (99% for both δ^2H and δ^{18}O; Table 3). The contribution of pre-event water at peak discharge showed increases from 6% to 99% for δ^2H and from 19% to 99% for δ^{18}O, as antecedent precipitation increased. The greatest pre-event contributions were usually observed during the recession limb of the hydrograph. Interestingly, the maximum pre-event water contribution was reached at peak discharge of Storm 5, despite the very high rainfall intensities of this storm and the high antecedent wetness conditions prevailing (API_7 = 185 mm; API_{14} = 311 mm).

[42] Overall, the difference between the pre-event fractions derived using δ^2H and δ^{18}O was small (2–10%; Table 3). The uncertainty in the derived pre-event water fractions (equation (5)) was 9% on average for δ^2H (range: 3–24%) and 16% for δ^{18}O (range: 2–31%). The largest uncertainty was associated with Storm 1, which showed a

Table 3. Pre-event Water Contributions to Storm Runoff Using One-Tracer, Two-Component Hydrograph Separation (δ^2H, δ^{18}O) and Corresponding Stream Water Flow Sources Derived From Two-Tracer, Three-Component Hydrograph Separation (δ^2H, δ^{18}O, and EC) Analyses

	Storm 1	Storm 2	Storm 3	Storm 4	Storm 5	Storm 6
			Pre-event Water			
δ^2H, %	31	79	72	88	99	92
δ^{18}O, %	38	81	66	93	99	88
			Flow Sources			
δ^2H and EC						
Rainfall, %	74	19	25	13	1	8
Soil water, %	18	26	25	2	9	5
Groundwater, %	8	55	50	85	90	87
δ^{18}O and EC						
Rainfall, %	73	17	29	8	2	14
Soil water, %	21	25	26	5	9	10
Groundwater, %	6	58	45	86	89	76

relatively small difference in the isotopic composition of its event and pre-event waters as compared to the other storms.

[43] Two-tracer three component hydrograph separation analysis (using δ^2H, δ^{18}O and EC) was consistent with the one-tracer calculations and showed that the runoff of Storm 1 consisted largely of rainfall (74% and 73% of the total storm runoff according to δ^2H and δ^{18}O, respectively; Table 3). Pre-event water in this first storm was small and consisted primarily of soil water (18% and 21% for δ^2H and δ^{18}O, respectively) showing its maximum contribution at the very end of the hydrograph recession limb. Following Storms 2 and 3, we found that rainwater sources declined and groundwater became the largest component of the pre-event water fraction (Table 3). Rainfall and soil water contributions in these storm events contributed to the rising limb of the hydrograph, whereas groundwater was mainly delivered during the falling limb. As the wetting-up cycle advanced, groundwater inputs to the stream further increased (Storm 4; Table 3), and their contributions were observed during the rising limb of the stream hydrograph showing its maximum at peak flow discharge. When antecedent wetness conditions were the highest, the storm runoff compositions were entirely pre-event water dominated and mostly groundwater (the runoff of Storms 5 and 6 consisted of 88 and 90% groundwater, respectively).

4.3. Soil and Stream Base Flow Transit Times

4.3.1. Temporal Variation of δ^2H and δ^{18}O

[44] Seasonal variation in precipitation isotope composition was high due to the occurrence of light rains associated with cold front passage during the dry season versus heavy storms brought by the easterly trade wind flow during the wet season (Figure 5a). Isotope ratios from rainfall, soil, and stream water all plotted on the local meteoric water line

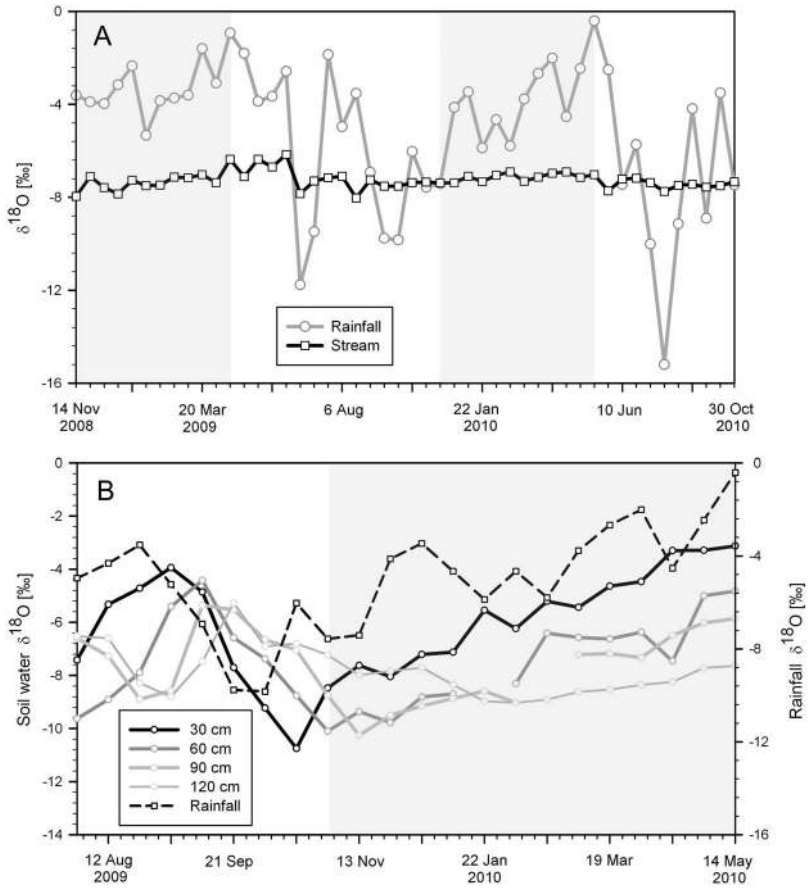

Figure 5. (a) Biweekly δ^{18}O values of base flow and corresponding volume weighted average values of rainfall between November 2008 and October 2010. (b) Weekly δ^{18}O values of soil water at the ridge top location (M1, Figure 1), and corresponding volume weighted average values of rainfall between August 2009 and May 2010. The gray shaded areas indicate the dry season periods.

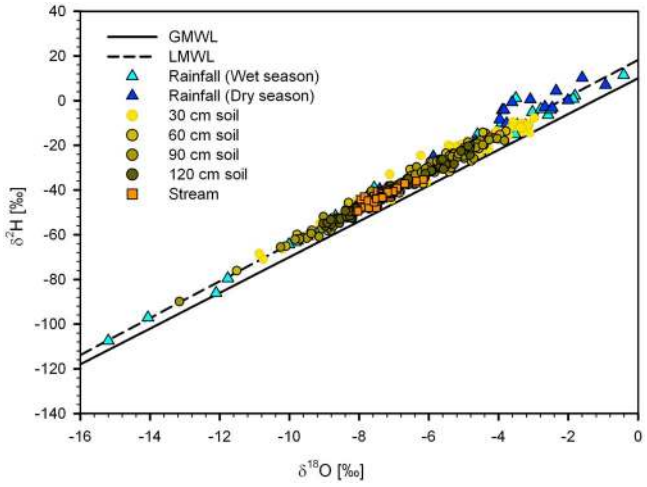

Figure 6. Isotope (δ^2H and δ^{18}O) signatures of rainfall, soil water (30, 60, 90, and 120 cm depth) and stream water. The local meteoric water line (LMWL; dashed line) is based on the 2008–2010 precipitation data and reads $\delta^2H = 8.25*\delta^{18}O + 18.20$; the solid line represents the global meteoric water line (GMWL): $\delta^2H = 8\delta^{18}O + 10$.

(LMWL) and showed no evidence of evaporative enrichment (Figure 6). Stream water δ^2H and δ^{18}O signatures followed the seasonal pattern as observed for rainfall but were strongly attenuated and damped. Biweekly volume weighted mean isotope values of precipitation ranged between −107.5‰ and 11.5‰ for δ^2H and −15.2‰ to −0.4‰ for δ^{18}O, meanwhile the range observed in stream water was only −49.5‰ to −35.3‰ for δ^2H and −8.0‰ to −6.2‰ for δ^{18}O. Soil water isotopic composition was progressively lagged and damped to rainfall with increasing soil depth. Soil water δ^2H ratios ranged in average between −66.2 and −9.9‰ and from −55.5 to −20.8‰ for 30 and 120 cm depths, respectively, meanwhile soil water δ^{18}O ranged between −10.2 and −3.1‰ and from −8.9 to −4.8‰ for 30 and 120 cm depths, respectively (Figure 5b).

4.3.2. Transit Time Estimates

[45] Soil water MTT at the shallowest depth was best estimated using the exponential transit time distribution model, whereas the MTTs at the deeper soil layers were best estimated using the dispersion distribution model. For the wet season months of August through October 2009, the transit time estimates for the 30 cm and 120 cm soil depths were 36 ± 10 days and 197 ± 67 days on average, respectively, across all hillslope locations. Soil water MTTs were also calculated for the full observation period (August 2009–May 2010, including a wet and a dry season), yielding 79 ± 10, 104 ± 43, 191 ± 97, and 228 ± 40 days for the 30, 60, 90, and 120 cm soil depths, respectively (data not shown). Overall, similar estimates of soil water residence times at different soil depths and locations were obtained using either δ^2H or δ^{18}O (Table 4). Across the hillslope, soil water showed a vertically aging through the profile, with no evidence of water aging in the downslope direction. The integrated response of the soil water tracer signal (TTD curves) at the different depths and locations within the hillslope are illustrated in Figure 7. The average model efficiency for all MTT soil water simulations across all locations was 0.40 and 0.44 (E) using δ^{18}O and δ^2H, respectively. The highest efficiencies (range: 0.46–0.71) were obtained for the shallower soil depths, whereas the poorest fits (range: 0.14–0.45) were observed for the deeper soil layers (Table 4).

[46] Stream base flow MTT was best estimated using the Gamma distribution model. The average MTT of stream

Table 4. Mean Transit Times and the Corresponding Model Parameters and Model Efficiencies for the Soil Water at Different Depths and at the Three Hillslope Positions (Figure 1) and the Base Flow[a]

	Model Parameters				Model Efficiency				
	MTT (days)		D_p		E		RMSE (‰)		
	δ^{18}O	δ^2H	δ^{18}O	δ^2H	δ^{18}O	δ^2H	δ^{18}O	δ^2H	Model
Soil									
			Upslope (M1)						
30 cm	20 (17,46)	36 (29,59)	-	-	0.52	0.51	1.5	9.9	EM
60	65 (42,86)	68 (43,93)	0.31 (0.12, 0.52)	0.31 (0.13, 0.50)	0.55	0.71	1.3	10.6	DM
90	91 (72,151)	360 (287, 434)	0.37 (0.19, 0.57)	0.66 (0.46, 0.85)	0.38	0.27	1.2	7.7	DM
120	139 (94,185)	(*)	0.38 (0.20, 0.56)	(*)	0.35	-	1.2	-	DM
			Midslope (M2)						
30 cm	43 (38,48)	51 (47, 55)	-	-	0.24	0.31	1.3	12.0	EM
60	79 (51, 112)	97 (62,132)	0.37 (0.17, 0.56)	0.40 (0.23, 0.59)	0.63	0.58	0.9	6.0	DM
90	130 (95, 167)	246 (203, 285)	0.52 (0.38, 0.67)	0.23 (0.12, 0.36)	0.32	0.45	1.1	8.3	DM
120	181 (144, 223)	270 (243, 297)	0.20 (0.15, 0.27)	0.11 (0.08, 0.14)	0.37	0.34	0.6	6.0	DM
			Downslope (M3)						
30 cm	32 (18,48)	36 (23,51)	-	-	0.46	0.51	1.1	11.6	EM
60	162 (125, 201)	153 (111, 195)	0.18 (0.13, 0.25)	0.17 (0.11, 0.24)	0.29	0.31	0.8	7.0	DM
90	298 (258, 333)	(*)	0.10 (0.05, 0.15)	(*)	0.14	-	1.0	-	DM
Stream			α, β	α, β					
	1083	958	0.60 (0.52, 0.72)	0.74 (0.70, 0.85)	0.51	0.53	0.3	1.5	GM
			1803 (804, 2772)	1299 (524, 1137)					

[a]Values in parenthesis are the 10th and 90th percentile values of the transit times estimates and the model parameters. D_p = dispersion parameter; α = shape parameter; β = scale parameter; EM = exponential model; DM = dispersion model; and GM = gamma model. Here MTT is the mean transit time, E is the Nash-Sutcliffe efficiency, RMSE is root mean square error. An asterisk means that no suitable model was found to fit the data.

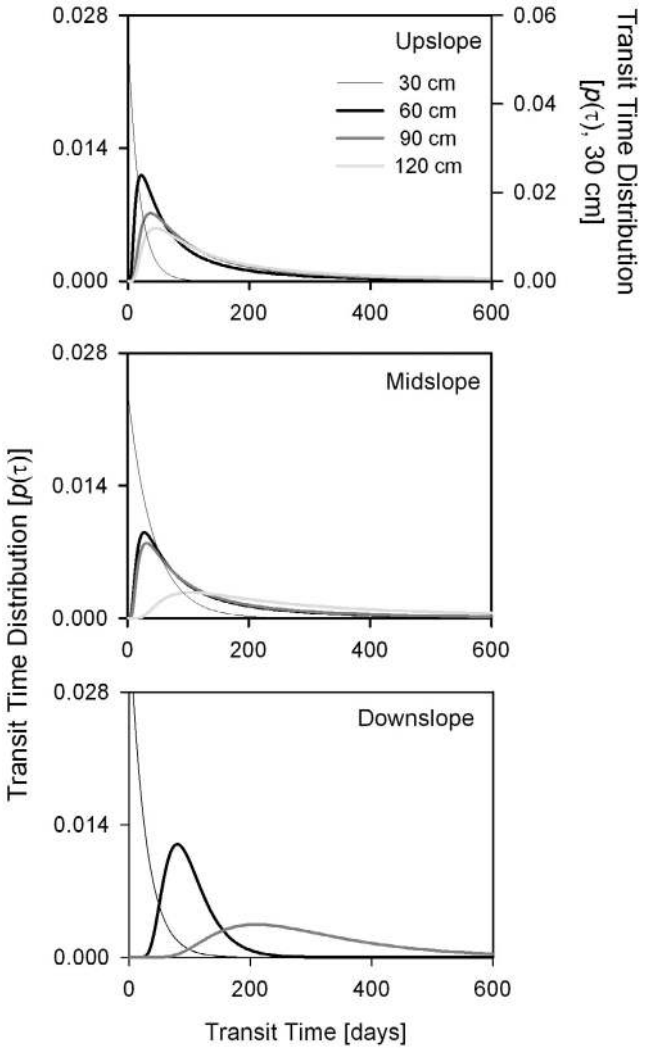

Figure 7. Soil water transit time distributions at different depths for the ridge top (M1), midslope (M2), and near-stream (M3) locations along the hillslope transect in the mature TMCF catchment. These curves were obtained based on best parameters estimates of the transit time distribution (TDD) models fitted along with their estimated soil water mean transit times.

base flow was 1021 ± 88 days (Table 4). The fit of the Gamma distribution to the observed isotopic stream water data was 0.52 on average. Table 4 provides further details on the values of the model parameters and the uncertainty bounds.

5. Discussion

5.1. A Different Type of Runoff Response for the Humid Tropics

[47] Unlike much of the past process-based hydrological research in steep, humid tropical montane regions that has observed rapid translation of rainfall to runoff via rapid lateral pathways at the near-surface soil [*Boy et al.*, 2008; *Goller et al.*, 2005; *Schellekens et al.*, 2004] or return flows as saturation overland flow [*Bonell et al.*, 1998; *Elsenbeer et al.*, 1994, 1995b], our results suggest that shallow lateral flow is not the dominant pathway of hillslope and catchment hydrological response at our site, despite the relatively high rain intensities observed for the storms analyzed ($I_{60\ max}$:16–63 mm/h). Rather, our combined hydrometric-isotopic-chemical tracer analysis suggests that vertical percolation of rainfall through the highly permeable volcanic soils and underlying substrate, and the progressive recharge of groundwater sources are the key hydrological processes controlling the amount, timing, and composition of subsurface storm runoff through the wetting-up cycle during the wet season. It is important to note also that the maximum rainfall intensities observed at our site are comparable with those reported in other humid tropical montane areas: 6–47 mm/h for the Luquillo Mountains, Puerto Rico (https://www.sas.upenn.edu/lczodata/) and 20–50 mm/h in Southeast Asia [*Chappell and Sherlock*, 2005].

[48] Isotope-inferred mean residence time estimates showed that soil water aged vertically up to 6 months through the ~120 cm soil profiles across all hillslope locations. In addition, soil water showed a lagged and damped isotopic response to rainfall with increasing soil depth. These findings suggest that infiltrating rainwater flows predominantly vertically through the soil to deeper layers where contributions to groundwater recharge are likely occurring by water that bypasses the soil matrix. This interpretation is supported by a recent isotope study by *Goldsmith et al.* [2012] at this site who found evidence of the presence of two distinct soil water pools: one highly mobile pool of precipitation that contributes to groundwater recharge and streamflow and a less mobile pool of water that contributes to plant fluxes [cf. *Brooks et al.*, 2010].

5.2. Progressive Changes in Amount and Composition of Storm Runoff Through Time

[49] We were able to examine six consecutive events to document the progressive change in amount and composition of storm runoff through time. This contrasts to most isotope-based analysis of stormflow generation in catchments to date that has come from single storm events [*Genereux*, 1998; *Goller et al.*, 2005; *McDonnell et al.*, 1990; *McGuire and McDonnell*, 2010; *Sklash et al.*, 1986; *Uchida et al.*, 2006] or a couple of events analyses during a wet season [*Elsenbeer et al.*, 1995a, 1995b; *Grimaldi et al.*, 2004; *Gomi et al.*, 2010; *McDonnell et al.*, 1991a, 1991b; *Schellekens et al.*, 2004]. Exceptions are the work of *Dewalle et al.* [1988], who sampled a sequence of six rain storms during the fall in a second-order catchment in Pennsylvania and observed a relative increase of soil water contributions related to increases in antecedent soil moisture conditions. *Brown et al.* [1999] was able to monitor five consecutive summer rain events in catchments located in the Castkill Mountains of New York, USA, and observed an increase in maximum event water contributions delivered from throughfall and shallow subsurface flow related directly to rainfall intensity. These limited sequential studies highlight the need (as noted by *Bonell* [1993, p. 253]) to "better understand the temporal variation on storm flow components and pathways and their incorporation in more physically based models."

[50] Our results showed a progressive change in runoff amount and timing through our monitored wetting-up cycle during the wet season, much like has been observed in temperate forested catchments with distinct seasonality in rainfall inputs [*Sidle et al.*, 2000; *McGuire and McDonnell*,

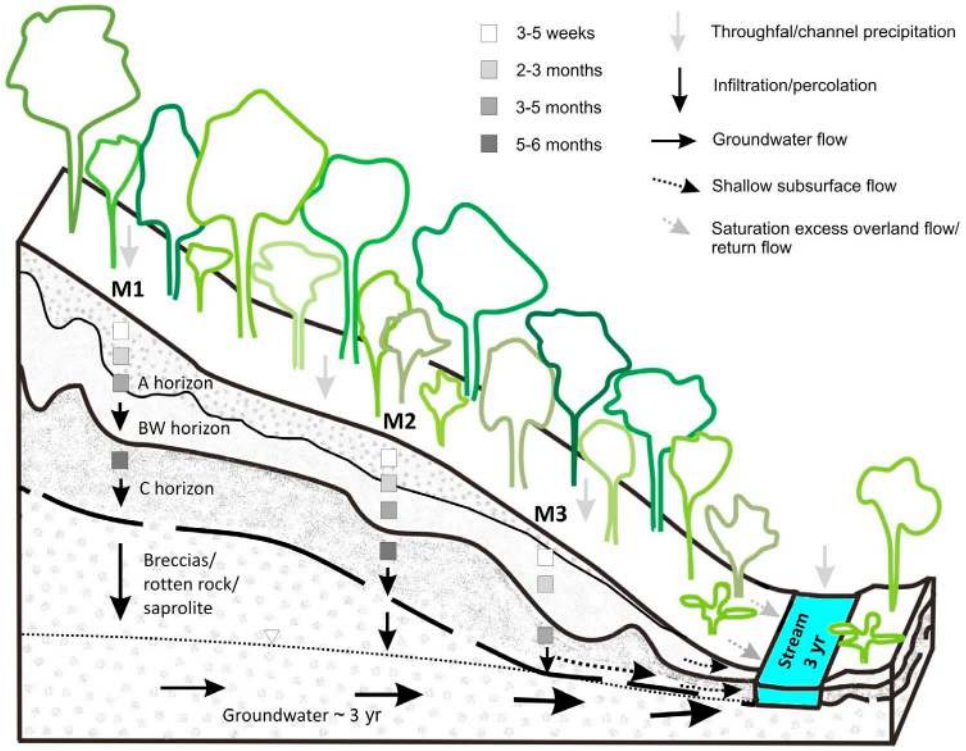

Figure 8. Conceptual model illustrating the variable flowpaths and mean water residence time contributing to stream runoff generation in the old-growth TMCF catchment.

2010; *Sayama et al.*, 2011]. Furthermore, the sequence of events sampled showed a striking pattern of increasing runoff composition through time, mapped onto a progressive change of stormflow sources from event to pre-event water dominance as antecedent wetness increased. Figure 8 shows a conceptual model for subsurface pathways and mean residence time of the water flow components contributing to runoff generation.

[51] We found that at low antecedent wetness conditions, the Q/P ratio for the first storm was very small and yielded high new event water volumes produced likely by direct channel precipitation (Figure 8). Soil surface dryness could have augmented this event water contribution via seasonal hydrophobicity that may have developed following the dry season (as noted by *Buttle and Turcotte* [1999]). This, combined with the high rainfall intensity of this first storm (33 mm/h; maximum I_{60}) likely contributed to produce some overland flow and/or pseudo overland flow [*McDonnell et al.*, 1991a, 1991b], resulting in the initial high event water response. *Blume et al.* [2008] has reported the effects of water repellency on event response dynamics and others have commented on hydrophobicity as a common phenomenon in volcanic ash soils [*Bachmann et al.*, 2000; *Poulenard et al.*, 2004].

[52] As catchment wetness progressed, new event water contributions to stormflow for the two consecutive rain storms diminished rapidly and shifted toward a dominance of pre-event water, where groundwater sources had the greatest contribution to flow. We observed increases of soil moisture content levels and establishment of groundwater tables in and around the near-stream valley extending upslope within our monitored groundwater well area to lower midslope hillslope positions. Although we lack measurements of the details of subsurface flow process response internal to the catchment, we hypothesize that the shallow sources were generated from subsurface flow at the near-stream valley areas along the stream channel, where hydraulic conductivities are reduced due to decreases in soil depth (Figure 8). The deeper flow contribution seems to be provided by groundwater from within the permeable weathered volcanic breccias-saprolite substrate (Figure 8), as the isotopic composition of sample groundwater from our wells completed in the permeable weathered volcanic breccias-saprolite was effectively the same in composition as stream base flow prior to the storm (see section 4.2.2).

[53] At high antecedent wetness, storm runoff response to the last 3 rain events produced the highest Q/P ratios and the highest pre-event water contributions, the latter of which were almost entirely dominated by groundwater sources. At this wetness stage, it is striking how the stream catchment reacted to the most intense rain event registered during the study period (Storm 5), categorized as an extreme event that occurs every 1–2 times during a year based on our 5-year observation period (F. Holwerda, unpublished data, 2012). Despite its short duration (~4 h), very high rain intensity (61 mm/h; maximum I_{60}) and the high antecedent precipitation conditions (API_{15} = 311 mm), the storm runoff was characterized by the highest observed groundwater contribution with no evidence of shallow stormflow sources.

5.3. How Old Are Soil Water and Stream Base Flow?

[54] Our soil MTT are the first such data that we are aware of from the humid tropics and show that soil water ages with increasing soil depth with no evidence of downslope aging (Figure 8). This is consistent with findings obtained by

Asano et al. [2002] and *McGuire and McDonnell* [2010] from temperate areas characterized by permeable soil layers; however, our soil water MTTs are much longer than these other investigations (<50 days [*Asano et al.*, 2002; *McGuire and McDonnell*, 2010]). This may be explained by differences in soil water sampling strategies and differences in soil structure. For example, *Asano et al.* [2002] collected the soil water every 2–3 weeks using pan-zero tension lysimeters in the Fudoji catchment, central Japan, while *McGuire and McDonnell* [2010] used suction lysimeters under tension of 40–50 kPa at daily to weekly time intervals in WS10 at the H. J. Andrews Experimental Forest in Oregon, USA. In our study, the soil water was collected at higher tension (60 kPa) on a weekly basis. On the other hand, our soils have shown capacities to store large amounts of water ($\sim$0.4 cm^3/cm^3 at wilting point (1500 kPa)[*Geris*, 2007]), a characteristic of highly stable aggregates of the volcanic ash soils.

[55] Stream base flow residence times estimated using δ^2H or $\delta^{18}O$ was on the order of 3 years, suggesting significant subsurface water storage capacity. Earlier work at the site found no evidence of interbasin transfer of water based on catchment water balance analysis [*Muñoz-Villers et al.*, 2012]. Further support for the latter is provided by the observation that the isotopic composition of the stream water falls within the range of values observed for rainfall (cf. Figure 6).

[56] Stream base flow residence times have not yet been reported for tropical montane cloud forest catchments. Our MTT estimates are longer than many values reported for forested headwater catchments (≤2 years [*Asano et al.*, 2002; *Burns et al.*, 2003; *McGlynn et al.*, 2003; *McGuire et al.*, 2005; *Roa-García and Weiler*, 2010]), although somewhat shorter compared to the Sourhope catchment in the Scottish Highlands, underlain by deeply and extensively fractured bedrock (4–5 years [*Hrachowitz et al.*, 2009; *Soulsby et al.*, 2009]).

[57] We present the stream base flow mean residence time with caution as without tritium-based characterization of the old component of base flow residence time, our 2.8 year estimated value is preliminary, since it likely underestimates the actual residence time of stream water at the site [*Stewart et al.*, 2010]. Hence future work in this TMCF catchment is needed to characterize the different stream base flow water stores using other more appropriate tracers.

6. Concluding Remarks

[58] We examined the runoff generation mechanisms of a steep, tropical montane cloud forest catchment underlying deep and permeable volcanic substrate in eastern Mexico using combined hydrometric-tracer field observations at different spatial and temporal scales and transit time modeling. We found that across a 6-week wetting-up cycle period in the 2009 wet season, runoff responses to rainfall were generally fast and showed a clear, progressive increase of pre-event water contribution from 35 to 99% of total stormflow with increasing stream discharge and antecedent wetness conditions. Stable isotope-inferred mean residence time estimates showed that soil water aged from 5 weeks at 30 cm to 6 months at 120 cm depth across the hillslope, with no evidence of aging in the downslope direction. Stream base flow mean residence time was greater than 2 years old, suggesting large catchment water storage capacity. These findings all suggest that shallow flowpaths are not the controlling process of catchment hydrological response at our site despite the relatively high rain intensities observed; rather, the high permeability of soils and substrate lead to rapid vertical rainfall percolation and recharge of deeper sources with rainfall-runoff responses dominated predominantly by groundwater discharge from within the hillslope.

[59] The implications of our results to land managers are important since one of the central ecosystem services attributed to TMCFs has been their contribution to dry season base flows, often associated to the lower evapotranspiration rates compared to non cloud-affected forests, and the extra water inputs gained via cloud water interception. Our work has shown that the high rainfall amounts prevailing in the wet season along with the high water percolation rates and high water subsurface potentials of this system are also important factors for dry season base flow sustenance and modulation of rainfall extremes related to climate change.

[60] **Acknowledgments.** We thank the Municipality of Coatepec (Veracruz, Mexico) and the residents of Loma Alta for permitting us to work in the La Cortadura Natural Reserve and its surroundings. We thank Tina Garland and Caroline Patrick for their assistance in analyzing the isotope samples. We would also like to thank Friso Holwerda for providing the rainfall data and for his comments on an earlier draft of the manuscript, Daniel Geissert for his assistance with the installation of the soil moisture stations, Cody Hale for helping with the transit time modeling, Chris Gabrielli for drilling the groundwater wells, and Adán Hernández and Sergio Cruz for their great assistance in the field. Finally, we appreciate the valuable comments of three anonymous reviewers and the Associate Editor that very much helped to improve an earlier version of the manuscript. Funding was provided by the U.S. National Science Foundation (NSF/DEB 0746179) and by CONACyT – Mexico (Repatriación Grant Program 170890).

References

Asano, Y., T. Uchida, and N. Ohte (2002), Residence times and flow paths of water in steep unchannelled catchments, Tanakami, Japan, *J. Hydrol.*, *261*(1–4), 173–192, doi:10.1016/S0022-1694(02)00005-7.

Bachmann, J., A. Ellies, and K. H. Hartge (2000), Development and application of a new sessile drop contact angle method to assess soil water repellency, *J. Hydrol.*, *231–232*, 66–75, doi:10.1016/S0022-1694(00)00184-0.

Báez, A. P., H. Padilla, J. Cervantes, D. Pereyra, and R. Belmont (1997), Rainwater chemistry at the eastern flanks of the Sierra Madre Oriental, Veracruz, Mexico, *J. Geophys. Res.*, *102*(D19), 23,329–23,336, doi:10.1029/97JD02077.

Blume, T., E. Zehe, D. E. Reusser, A. Iroume, and A. Bronstert (2008), Investigation of runoff generation in a pristine, poorly gauged catchment in the Chilean Andes I: A multi-method experimental study, *Hydrol. Processes*, *22*(18), 3661–3675, doi:10.1002/hyp.6971.

Bonell, M. (1993), Progress in the understanding of runoff generation dynamics in forests, *J. Hydrol.*, *150*(2–4), 217–275, doi:10.1016/0022-1694(93)90112-M.

Bonell, M. (2005), Runoff generation in tropical forests, in *Forests, Water and People in the Humid Tropics*, edited by M. Bonell and L. A. Bruijnzeel, pp. 314–406, Cambridge Univ. Press, Cambridge, U.K., doi:10.1017/CBO9780511535666.020.

Bonell, M., and D. A. Gilmour (1978), Development of overland flow in a tropical rainforest catchment, *J. Hydrol.*, *39*(3–4), 365–382, doi:10.1016/0022-1694(78)90012–4.

Bonell, M., C. J. Barnes, C. R. Grant, A. Howard, and J. Burns Scatena (1998), High rainfall response-dominated catchments: A comparative study of experiments in tropical north-east Queensland with temperate New Zealand, in *Isotope Tracers in Catchment Hydrology*, edited by C. Kendall and J. J. McDonnell, pp. 347–390, Elsevier, Amsterdam, The Netherlands.

Boy, J., C. Valarezo, and W. Wilcke (2008), Water flow paths in soil control element exports in an Andean tropical montane forest, *Eur. J. Soil Sci.*, *59*(6), 1209–1227, doi:10.1111/j.1365-2389.2008.01063.x.

Brooks, J. R., H. R. Barnard, R. Coulombe, and J. J. McDonnell (2010), Ecohydrologic separation of water between trees and streams in a Mediterranean climate, *Nat. Geosci.*, *3*, 101–104, doi:10.1038/ngeo722.

Brown, V. A., J. J. McDonnell, D. A. Burns, and C. Kendall (1999), The role of event water, a rapid shallow flow component, and catchment size in summer stormflow, *J. Hydrol.*, *217*(3–4), 171–190, doi:10.1016/S0022-1694(98)00247-9.

Bruijnzeel, L. A., and F. N. Scatena (2011), Hydrometeorology of tropical montane cloud forests Preface, *Hydrol. Processes*, *25*(3), 319–326, doi:10.1002/hyp.7962.

Bruijnzeel, L. A., M. Kappelle, M. Mulligan, and F. N. Scatena (2010), Tropical montane cloud forests: State of knowledge and sustainability perspectives in a changing world, in *Tropical Montane Cloud Forests. Science for Conservation and Management*, edited by L. A. Bruijnzeel et al., pp. 691–740, Cambridge Univ. Press, Cambridge, U.K., doi:10.1017/CBO9780511778384.074.

Burns, D. A., et al. (2003), The geochemical evolution of Riparian ground water in a forested Piedmont catchment, *Ground Water*, *41*(7), 913–925, doi:10.1111/j.1745-6584.2003.tb02434.x.

Buttle, J. M., and D. S. Turcotte (1999), Runoff processes on a forested slope on the Canadian Shield, *Nord. Hydrol.*, *30*(1), 1–20.

Calder, I. R., and C. H. R. Kidd (1978), Note on the dynamic calibration of tipping-bucket gauges, *J. Hydrol.*, *39*(3–4), 383–386, doi:10.1016/0022-1694(78)90013-6.

Campos, A. (2010), Response of soil inorganic nitrogen to land use and topographic position in the Cofre de Perote Volcano (Mexico), *Environ. Manage. N. Y.*, *46*(2), 213–224, doi:10.1007/s00267-010-9517-z.

Castillo–Campos, G., J. G. García Franco, K. Mehltreter, and M. L. Martínez (2009), Registros nuevos de *Ponthieva brenesii* (Orchidaceae) y *Piper xanthostachyum* (Piperaceae) para el estado de Veracruz, México, *Rev. Mex. Biodiversidad*, *80*(2), 565–569.

Chappell, N. A., and M. D. Sherlock (2005), Contrasting flow pathways within tropical forest slopes of Ultisol soils, *Earth Surf. Processes Landforms*, *30*(6), 735–753, doi:10.1002/esp.1173.

Cuartas, L. A., J. Tomasella, A. D. Nobre, M. G. Hodnett, M. J. Waterloo, and J. C. Munera (2007), Interception water-partitioning dynamics for a pristine rainforest in Central Amazonia: Marked differences between normal and dry years, *Agric. For. Meteorol.*, *145*(1–2), 69–83, doi:10.1016/j.agrformet.2007.04.008.

Dewalle, D. R., B. R. Swistock, and W. E. Sharpe (1988), 3-component tracer model for stormflow on a small Appalachian forested catchment, *J. Hydrol.*, *104*(1–4), 301–310, doi:10.1016/0022-1694(88)90171-0.

Dykes, A. P., and J. B. Thornes (2000), Hillslope hydrology in tropical rainforest steeplands in Brunei, *Hydrol. Processes*, *14*(2), 215–235, doi:10.1002/(SICI)1099-1085(20000215)14:2<215::AID-HYP921>3.0.CO;2-P.

Elsenbeer, H., and R. A. Vertessy (2000), Stormflow generation and flowpath characteristics in an Amazonian rainforest catchment, *Hydrol. Processes*, *14*(14), 2367–2381, doi: 10.1002/1099-1085(20001015)14:14<2367::AID-HYP107>3.0.CO;2-H.

Elsenbeer, H., A. West, and M. Bonell (1994), Hydrologic pathways and stormflow hydrochemistry at south creek, northeast Queensland, *J. Hydrol.*, *162*(1–2), 1–21, doi:10.1016/0022-1694(94)90002-7.

Elsenbeer, H., A. Lack, and K. Cassel (1995a), Chemical fingerprints of hydrological compartments and flow paths at La Cuenca, western Amazonia, *Water Resour. Res.*, *31*(12), 3051–3058, doi:10.1029/95WR02537.

Elsenbeer, H., D. Lorieri, and M. Bonell (1995b), Mixing model approaches to estimate storm flow sources in an overland flow-dominated tropical rain-forest catchment, *Water Resour. Res.*, *31*(9), 2267–2278, doi:10.1029/95WR01651.

Freer, J., K. Beven, and B. Ambroise (1996), Bayesian estimation of uncertainty in runoff prediction and the value of data: An application of the GLUE approach, *Water Resour. Res.*, *32*(7), 2161–2173, doi:10.1029/95WR03723.

Fritsch, J. M. (1992), Les effets du dl'hydrologie de petits bassins versants, Ph.D. thesis, Universitllier, location?, France.

Gabrielli, C. P., and J. J. McDonnell (2011), An inexpensive and portable drill rig for bedrock groundwater studies in headwater catchments, *Hydrol. Process.*, *26*(4), 622–632, doi:10.1002/hyp.8212.

Garcia, E. (1988), Modificaciones al istema de clasificación climática de Köppen, 217 pp., Offset Larios, México, D. F., México.

García-Franco, J. G., G. Castillo-Campos, K. Mehltreter, M. L. Martínez, and G. Vázquez (2008), Composición florística de un bosque mesófilo del centro de Veracruz, México, *Bol. Soc. Bot. Mex.*, *83*, 37–52.

Gash, J. H. C. (1979), Analytical model of rainfall interception by forests, *Q. J. R. Meteorol. Soc.*, *105*(443), 43–55, doi:10.1002/qj.49710544304.

Geissert, D. (1999), Regionalización geomorfológica del estado de Veracruz, *Invest. Geogr.*, *40*, 23–47.

Genereux, D. (1998), Quantifying uncertainty in tracer-based hydrograph separations, *Water Resour. Res.*, *34*(4), 915–919, doi:10.1029/98WR00010.

Geris, J. (2007), Changes in soil physical characteristics, infiltration and hill slope hydrological response associated with forest conversion to pasture in Central Veracruz, Mexico. M.S. thesis, VU Univ., Amsterdam, Netherlands.

Goldsmith, G. R., L. E. Muñoz-Villers, F. Holwerda, J. J. McDonnell, H. Asbjornsen, and T. E. Dawson (2012), Stable isotopes reveal linkages among ecohydrological processes in a seasonally dry tropical montane cloud forest, *Ecohydrology*, doi:10.1002/eco.268, in press.

Goller, R., W. Wilcke, M. J. Leng, H. J. Tobschall, K. Wagner, C. Valarezo, and W. Zech (2005), Tracing water paths through small catchments under a tropical montane rain forest in south Ecuador by an oxygen isotope approach, *J. Hydrol.*, *308*(1–4), 67–80, doi:10.1016/j.jhydrol.2004.10.022.

Gomi, T., Y. Asano, T. Uchida, Y. Onda, R. C. Sidle, S. Miyata, K. Kosugi, S. Mizugaki, T. Fukuyama, and T. Fukushima (2010), Evaluation of storm runoff pathways in steep nested catchments draining a Japanese cypress forest in central Japan: A geochemical approach, *Hydrol. Processes*, *24*(5), 550–566, doi:10.1002/hyp.7550.

Grimaldi, C., M. Grimaldi, A. Millet, T. Bariac, and J. Boulegue (2004), Behaviour of chemical solutes during a storm in a rainforested headwater catchment, *Hydrol. Processes*, *18*(1), 93–106, doi:10.1002/hyp.1314.

Hamilton, L. S., J. O. Juvik, and F. N. Scatena (1995), The Puerto Rico Tropical Montane Cloud Forest Symposium: Introduction and workshop synthesis, in *Tropical Montane Cloud Forests*, edited by L. S. Hamilton et al., pp. 1–16, Springer, New York.

Hewlett, J. D., and A. R. Hibbert (1967), Factors affecting the response of small watersheds to precipitation in humid areas, in *Forest Hydrology*, edited by W. E. Sopper and H. W. Lull, pp. 275–290, Pergamon Press, Oxford, U. K.

Holwerda, F., F. N. Scatena, and L. A. Bruijnzeel (2006), Throughfall in a Puerto Rican lower montane rain forest: A comparison of sampling strategies, *J. Hydrol.*, *327*(3–4), 592–602, doi:10.1016/j.jhydrol.2005.12.014.

Holwerda, F., L. A. Bruijnzeel, L. E. Munoz-Villers, M. Equihua, and H. Asbjornsen (2010), Rainfall and cloud water interception in mature and secondary lower montane cloud forests of central Veracruz, Mexico, *J. Hydrol.*, *384*(1–2), 84–96, doi:10.1016/j.jhydrol.2010.01.012.

Hrachowitz, M., C. Soulsby, D. Tetzlaff, I. A. Malcolm, and G. Schoups (2010), Gamma distribution models for transit time estimation in catchments: Physical interpretation of parameters and implications for time-variant transit time assessment, *Water Resour. Res.*, *46*, W10536, doi:10.1029/2010WR009148.

Hrachowitz, M., C. Soulsby, D. Tetzlaff, J. J. C. Dawson, S. M. Dunn, and I. A. Malcolm (2009), Using long-term data sets to understand transit times in contrasting headwater catchments, *J. Hydrol.*, *367*(3–4), 237–248, doi:10.1016/j.jhydrol.2009.01.001.

Jencso, K. G., B. L. McGlynn, M. N. Gooseff, K. E. Bencala, and S. M. Wondzell (2010), Hillslope hydrologic connectivity controls riparian groundwater turnover: Implications of catchment structure for riparian buffering and stream water sources, *Water Resour. Res.*, *46*, W10524, doi:10.1029/2009WR008818.

Karlsen, R. (2010), Stormflow processes in a mature tropical montane cloud forest catchment, Coatepec, Veracruz, Mexico. M.S. thesis, VU Univ., Amsterdam, Netherlands.

Kennedy, V. C., G. W. Zellweger, and R. J. Avanzino (1979), Variation of rain chemistry during storms at 2 sites in northern California, *Water Resour. Res.*, *15*(3), 687–702, doi:10.1029/WR015i003p00687.

Kirchner, J. W., X. H. Feng, and C. Neal (2001), Catchment-scale advection and dispersion as a mechanism for fractal scaling in stream tracer concentrations, *J. Hydrol.*, *254*(1–4), 82–101, doi:10.1016/S0022-1694(01)00487-5.

Kreft, A., and A. Zuber (1978), Physical meaning of dispersion-equation and its solutions for different initial and boundary-conditions, *Chem. Eng. Sci.*, *33*(11), 1471–1480, doi:10.1016/0009-2509(78)85196-3.

Laudon, H., and O. Slaymaker (1997), Hydrograph separation using stable isotopes, silica and electrical conductivity: An alpine example, *J. Hydrol.*, *201*(1–4), 82–101, doi:10.1016/S0022-1694(97)00030-9.

Lawton, R. O., U. S. Nair, R. A. Pielke, and R. M. Welch (2001), Climatic impact of tropical lowland deforestation on nearby montane cloud forests, *Science*, *294*(5542), 584–587.

Levia, D. F., D. Carlyle-Moses, and T. Tadashi (Eds.) (2011), *Forest Hydrology and Biogeochemistry: Synthesis of Past Research and Future Directions, Ecol. Stud. Ser.*, vol. 216, 740 pp., Springer, Heidelberg, Germany.

Lyon, S. W., S. L. E. Desilets, and P. A. Troch (2008), Characterizing the response of a catchment to an extreme rainfall event using hydrometric and isotopic data, *Water Resour. Res.*, *44*, W06413, doi:10.1029/2007WR006259.

Maloszewski, P., and A. Zuber (1982), Determining the turnover time of groundwater systems with the aid of environmental tracers. 1. models and their applicability, *J. Hydrol.*, *57*(3–4), 207–231, doi:10.1016/0022-1694(82)90147-0.

Maloszewski, P., and A. Zuber (1993), Tracer experiments in fractured rocks: Matrix diffusion and validity of models, *Water Resour. Res.*, *29*(8), 2723–2735, doi:10.1029/93WR00608.

Marín-Castro, B. E. (2010), Variación espacial de la conductividad hidráulica saturada en suelos de origen volcánico bajo tres usos de suelo en el centro de Veracruz, México. M.S. thesis, Posgrado en Ciencias, Inst. de Ecol., A.C., Xalapa, Veracruz, México.

McDonnell, J. J., M. Bonell, M. K. Stewart, and A. J. Pearce (1990), Deuterium variations in storm rainfall - Implications for stream hydrograph separation, *Water Resour. Res.*, *26*(3), 455–458, doi:10.1029/WR026i003p00455.

McDonnell, J. J., I. F. Owens, and M. K. Stewart (1991a), A case study of shallow flow paths in a steep zero-order basin: A physical-chemical-isotopic analysis, *Water Resour. Bull.*, *27*(4), 679–685, doi:10.1111/j.1752-1688.1991.tb01469.x.

McDonnell, J. J., M. K. Stewart, and I. F. Owens (1991b), Effect of catchment-scale subsurface mixing on stream isotopic response, *Water Resour. Res.*, *27*(12), 3065–3073, doi:10.1029/91WR02025.

McGlynn, B. L., J. J. McDonnell, M. K. Stewart, and J. Seibert (2003), On the relationships between catchment scale and streamwater mean residence time, *Hydrol. Processes*, *17*(1), 175–181, doi:10.1002/hyp.5085.

McGuire, K. J., and J. J. McDonnell (2006), A review and evaluation of catchment transit time modeling, *J. Hydrol.*, *330*(3–4), 543–563, doi:10.1016/j.jhydrol.2006.04.020.

McGuire, K. J., and J. J. McDonnell (2010), Hydrological connectivity of hillslopes and streams: Characteristic time scales and nonlinearities, *Water Resour. Res.*, *46*, W10543, doi:10.1029/2010WR009341.

McGuire, K. J., J. J. McDonnell, M. Weiler, C. Kendall, B. L. McGlynn, J. M. Welker, and J. Seibert (2005), The role of topography on catchment-scale water residence time, *Water Resour. Res.*, *41*, W05002, doi:10.1029/2004WR003657.

Muñoz-Villers, L. E. (2008), Efecto del cambio en el uso de suelo sobre la dinámica hidrológica y calidad de agua en el trópico húmedo del centro de Veracruz, México. Ph.D. thesis, Univ. Autónoma Metropolitana, México D.F., México.

Muñoz-Villers, L. E., and J. López-Blanco (2008), Land use/cover changes using Landsat TM/ETM images in a tropical and biodiverse mountainous area of central eastern Mexico, *Int. J. Remote Sens.*, *29*(1), 71–93, doi:10.1080/01431160701280967.

Muñoz-Villers, L. E., F. Holwerda, M. Gómez-Cárdenas, M. Equihua, H. Asbjornsen, L. A. Bruijnzeel, B. E. Marín-Castro, and C. Tobón (2012), Water balances of old-growth and regenerating montane cloud forests in central Veracruz, Mexico, *J. Hydrol.*, *462-463*, 53–66, doi:10.1016/j.jhydrol.2011.01.062.

Nash, J. E., and J. V. Sutcliffe (1970), River flow forecasting through conceptual models, I, A discussion of principles, *J. Hydrol.*, *10*(3), 282–290, doi:10.1016/0022-1694(70)90255-6.

Niedzialek, J. M., and F. L. Ogden (2010), First-order catchment mass balance during the wet season in the Panama Canal Watershed, *J. Hydrol.*, *462-463*, 77–86, doi:10.1016/j.jhydrol.2010.07.044.

Noguchi, S., A. R. Nik, B. Kasran, M. Tani, T. Sammori, and K. Morisada (1997), Soil physical properties and preferential flow pathways in tropical rain forest, Bukit Tarek, Peninsular Malaysia, *J. For. Res.*, *2*(2), 115–120, doi:10.1007/BF02348479.

Ogunkoya, O. O., and A. Jenkins (1993), Analysis of storm hydrograph and flow pathways using a 3-component hydrograph separation model, *J. Hydrol.*, *142*(1–4), 71–88, doi:10.1016/0022-1694(93)90005-T.

Pinder, G. F., and J. F. Jones (1969), Determination of ground-water component of peak discharge from chemistry of total runoff, *Water Resour. Res.*, *5*(2), 438–445, doi: 10.1029/WR005i002p00438.

Poulenard, J., J. C. Michel, F. Bartoli, J. M. Portal, and P. Podwojewski (2004), Water repellency of volcanic ash soils from Ecuadorian paramo: Effect of water content and characteristics of hydrophobic organic matter, *Eur. J. Soil Sci.*, *55*(3), 487–496, doi:10.1111/j.1365-2389.2004.00625.x.

Pounds, J. A., et al. (2006), Widespread amphibian extinctions from epidemic disease driven by global warming, *Nature*, *439*(7073), 161–167, doi:10.1038/nature04246.

Ray, D. K., U. S. Nair, R. O. Lawton, R. M. Welch, and R. A. Pielke (2006), Impact of land use on Costa Rican tropical montane cloud forests: Sensitivity of orographic cloud formation to deforestation in the plains, *J. Geophys. Res.*, *111*, D02108, doi:10.1029/2005JD006096.

Roa-García, M. C., and M. Weiler (2010), Integrated response and transit time distributions of watersheds by combining hydrograph separation and long-term transit time modeling, *Hydrol. Earth Syst. Sci.*, *14*(8), 1537–1549, doi:10.5194/hess-14-1537-2010.

Saunders, T. J., M. E. McClain, and C. A. Llerena (2006), The biogeochemistry of dissolved nitrogen, phosphorus, and organic carbon along terrestrial-aquatic flowpaths of a montane headwater catchment in the Peruvian Amazon, *Hydrol. Processes*, *20*(12), 2549–2562, doi:10.1002/hyp.6215.

Sayama, T., J. J. McDonnell, A. Dhakal, and K. Sullivan (2011), How much water can a watershed store?, *Hydrol. Proc.*, *25*(25), 3899–3908, doi:10.1002/hyp.8288.

Schellekens, J., F. N. Scatena, L. A. Bruijnzeel, A. van Dijk, M. M. A. Groen, and R. J. P. van Hogezand (2004), Stormflow generation in a small rainforest catchment in the Luquillo experimental forest, Puerto Rico, *Hydrol. Processes*, *18*(3), 505–530, doi:10.1002/hyp.1335.

Seibert, J., and J. J. McDonnell (2010), Land-cover impacts on streamflow: A change- detection modelling approach that incorporates parameter uncertainty, *Hydrol. Sci. J.*, *55*(3), 316–332, doi:10.1080/02626661003683264.

Sidle, R. C., Y. Tsuboyama, S. Noguchi, I. Hosoda, M. Fujieda, and T. Shimizu (2000), Stormflow generation in steep forested headwaters: A linked hydrogeomorphic paradigm, *Hydrol. Processes*, *14*, 369–385, doi:10.1002/(SICI)1099-1085(20000228)14:3<369::AID-HYP943>3.0.CO;2-P.

Sistema Meteorológico Nacional (2009a), Llega "El Niño"; se estima que continuará durante el invierno de 2009–10, comunicado del 16 de julio de 2009, Delegacion Miguel Hidalgo, México.

Sistema Meteorológico Nacional (2009b), El mes de julio de 2009, segundo más seco del periodo 1941–2009, comunicado del 4 de agosto de 2009, Delegacion Miguel Hidalgo, México.

Sklash, M. G., and R. N. Farvolden (1979), Role of groundwater in storm runoff, *J. Hydrol.*, *43*(1–4), 45–65, doi:10.1016/0022-1694(79)90164-1.

Sklash, M. G., M. K. Stewart, and A. J. Pearce (1986), Storm runoff generation in humid headwater catchments. 2. A case-study of hillslope and low-order stream response, *Water Resour. Res.*, *22*(8), 1273–1282, doi:10.1029/WR022i008p01273.

Soulsby, C., D. Tetzlaff, and M. Hrachowitz (2009), Tracers and transit times: Windows for viewing catchment scale storage?, *Hydrol. Processes*, *23*, 3503–3507, doi:10.1002/hyp.7501.

Starr, J. L., and I. C. Palineanu (2002), Methods for measurement of soil water content: Capacitance devices, in *Methods of Soil Analysis: Part 4 Physical Methods*, edited by J. H. Dane and G. C. Topp, pp. 463–474, Soil Sci. Soc. of Am., Madison, Wisc.

Stewart, M. K., and J. J. McDonnell (1991), Modeling base-flow soil-water residence times from deuterium concentrations, *Water Resour. Res.*, *27*(10), 2681–2693, doi:10.1029/91WR01569.

Stewart, M. K., J. Mehlhorn, and S. Elliott (2007), Hydrometric and natural tracer (oxygen-18, silica, tritium and sulphur hexafluoride) evidence for a dominant groundwater contribution to Pukemanga Stream, New Zealand, *Hydrol. Processes*, *21*(24), 3340–3356, doi:10.1002/hyp.6557.

Stewart, M. K., U. Morgenstern, and J. J. McDonnell (2010), Truncation of stream residence time: How the use of stable isotopes has skewed our concept of streamwater age and origin, *Hydrol. Processes*, *24*(12), 1646–1659, doi:10.1002/hyp.7576.

Takahashi, T., and S. Shoji (2002), Distribution and classification of volcanic ash soils, *Global Environ. Res.*, *6*, 83–97.

Tobón, C., L. A. Bruijnzeel, F. K. A. Frumau, and J. C. Calvo-Alvardo (2010), Changes in soil physical properties after conversion of tropical montane cloud forest to pasture in northern Costa Rica, in *Tropical Montane Cloud Forests. Science for Conservation and Management*, edited by L. A. Bruijnzeel et al., pp. 502–515, Cambridge Univ. Press, Cambridge, U.K., doi:10.1017/CBO9780511778384.054.

Tognetti, S., B. Aylward, and L. A. Bruijnzeel (2010), Assessment needs to support the development of arrangements for payments for ecosystem services from tropical montane cloud forests, in *Tropical Montane Cloud Forests. Science for Conservation and Management*, edited by L. A. Bruijnzeel et al., pp. 671–685, Cambridge Univ. Press, Cambridge, U.K, doi:10.1017/CBO9780511778384.072.

Uchida, T., J. J. McDonnell, and Y. Asano (2006), Functional intercomparison of hillslopes and small catchments by examining water source, flowpath and mean residence time, *J. Hydrol.*, *327*(3–4), 627–642, doi:10.1016/j.jhydrol.2006.02.037.

Viessman, W., G. L. Lewis, and J. W. Knapp (1989), *Introduction to Hydrology*, HarperCollins, New York.

Weiler, M., B. L. McGlynn, K. J. McGuire, and J. J. McDonnell (2003), How does rainfall become runoff? A combined tracer and runoff transfer function approach, *Water Resour. Res.*, *39*(11), 1315, doi:10.1029/2003WR002331.

Zadroga, F. (1981), The hydrological importance of a montane cloud forest area of Costa Rica, in *Tropical Agricultural Hydrology*, edited by R. Lal and E. W. Russell, pp. 59–73, John Wiley, New York.